Final Report

# LATERAL STABILITY OF LIGHT TRUSSES AND OPEN WEB STEEL JOISTS

by

Raed Tolaymat

and

Thomas M. Murray
Principal Investigator

Submitted to

VULCRAFT
A Division at NUCOR Corporation
Norfolk, Nebraska

Report No. FSEL/VULCRAFT 84-01

June 1984

FEARS STRUCTURAL ENGINEERING LABORATORY
School of Civil Engineering and Environmental Science
University of Oklahoma
Norman, Oklahoma 73019

ACKNOWLEDGEMENTS

This study was sponsored by VULCRAFT, a Division of NUCOR Corporation through their Fellowship Program. This financial assistance is sincerely appreciated, especially by the junior author. The help of Mr. Marcus Withiam and Mr. Hassan Mukayed in preparing the report is acknowledged with sincere appreciation.

## ABSTRACT

This study involves the development of two methodologies for the design and analysis of light trusses and open web steel joists supporting standing seam roof systems. The primary mode of failure considered in the study is out-of-plane lateral buckling of the compression chords of these structural members. The first method considers the behavior of joists and trusses in conjunction with standing seam roof system components. The second method studies the behavior of trusses and joists without standing seam roof system components but includes web restraint effects.

A series of experimental tests conducted prior to this study serves as a basis of comparison for results from both analytical methods. A design equation is developed based on the method that was found to give better results. The design equation results are compared to theoretical and experimental results.

Based on the experimental research and on the findings from this study, recommendations are made for best use of a simple design equation and safer construction of standing seam roofs supported by light trusses and open web steel joists.

TABLE OF CONTENTS

LIST OF FIGURES

LIST OF TABLES

## NOMENCLATURE

$A$ = top chord cross-sectional area

$B$ = maximum lateral deflection of the buckled top chord

$C_1$ = constant relating to joist chord configuration

$C_2$ = constant relating to number of rows of bridging

$C_c = \sqrt{2\pi^2 E/QF_y}$, proportional limit slenderness ratio

$CF$ = clip coefficient of friction

$C_m$ = moment reduction factor

$E$ = modulus of elasticity

$F_a$ = allowable axial unit compressive stress

$F_b$ = allowable bending unit compressive stress

$F'_e$ = elastic allowable axial unit compressive stress

$FF$ = friction force provided by one clip

$I_y$ = moment of inertia of the top chord about the vertical axis

$I_w$ = moment of inertia of one web member about a horizontal axis in the plane of the joist

$K$ = total stiffness of web members at each panel point

$L$ = joist span

$L_w$ = length of one web member

$M$ = bending moment

$M_{max}$ = bending moment at midspan

$NF$ = normal force applied on a single clip

$P$ = top chord axial force

$P_{cr}$ = top chord buckling load

$P_e$ = elastic top chord buckling load

$P_I$ = inelastic top chord buckling load

$P_p$ = proportional limit load

$P_y$ = chord yield load

$Q$ = a form factor equal to unity unless the width/thickness ratio of one or more elements of the profile exceeds the limits specified in the AISC specifications section 1.9 for hot rolled sections and in the AISI specifications section 3 for cold formed sections

$S$ = bridging spacing

$U$ = internal bending strain energy due to bending

$V$ = shear force

$W$ = external work done by frictional forces due to buckling

$a$ = factor that depends on top chord axial load variation

$b$ = factor that depends on the number of panel points between bridging lines

$c$ = factor that depends on web component type, rod or angle

$d$ = effective joist depth

$f_a$ = computed axial unit compressive stress

$f_b$ = computed bending unit compressive stress

$h$ = region width in modified Newmark's method

$(kS/r)_y$ = slenderness ratio of top chord with respect to the vertical axis

$k_w$ = lateral stiffness of one web member

$n$ = number of clips acting on top chord between bridging lines

$p$ = distance between panel points

$r$ = least radius of gyration of top or bottom chords

$s'$ = standing seam roof clip spacing

$w$ = uniform load applied on one joist, equal to roof load per unit area times joist spacing

$w_A$ = predicted joist failure load using the design equation

$w_E$ = experimental failure load

$w_T$ = predicted joist failure load using modified Newmark's method

$x$ = distance from left support to studied point

$y'$ = first derivative of top chord lateral deflection function with respect to x

$y''$ = second derivative of top chord lateral deflection function with respect to x

# LATERAL STABILITY OF LIGHT TRUSSES AND OPEN WEB STEEL JOISTS

## CHAPTER I

## INTRODUCTION

### 1.1 Background

Unlike conventional roof systems, standing seam roof systems do not provide lateral support to the top chords of trusses and steel joists by direct mechanical connection. Consequently, the load carrying capacity of these structural members may be lessened. With conventional roof systems, defined here as roof cladding composed of steel cold-formed sheets attached to supporting members with steel fasteners which do not permit longitudinal movement of the sheets, lateral support is provided at each fastener location, Figure 1.1(a). The fasteners are usually spaced 12 in. to 36 in. apart, and the Steel Joist Institute (SJI) specifications for open web steel joists supporting conventional deck[1] allows the designer to assume full lateral support if the fastener spacing is less than or equal to 36 in. Thus, the failure modes associated with joist top chords for this type of construction is limited to yielding, in-plane column buckling and local buckling. With standing seam roof systems, sliding clips are used to connect the steel

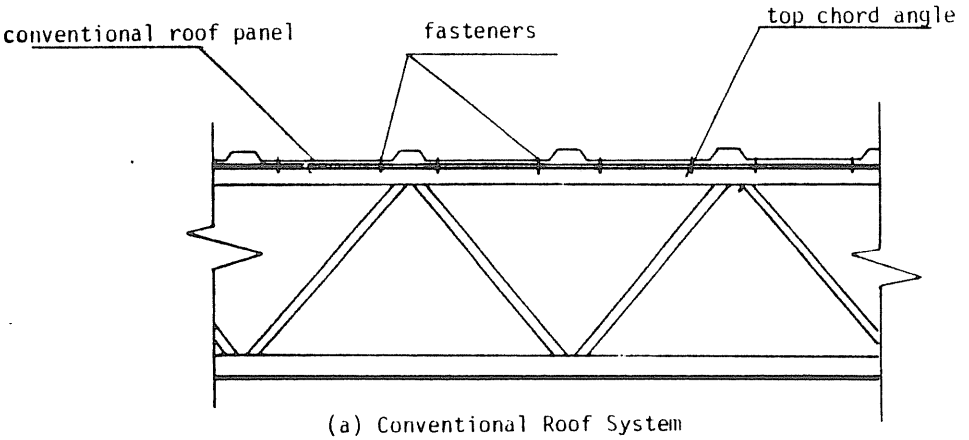


(a) Conventional Roof System

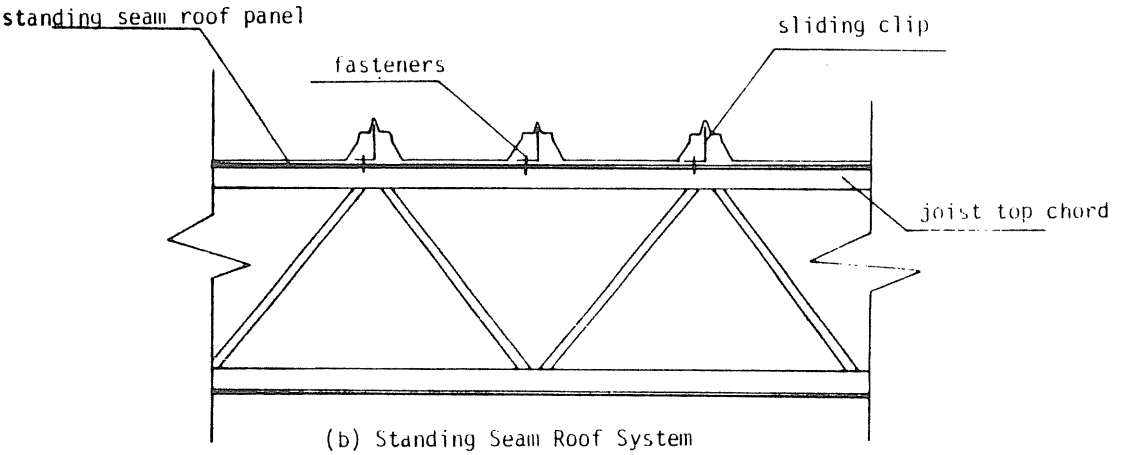


(b) Standing Seam Roof System

Figure 1.1 Conventional and Standing Seam Roof Systems

sheets to supporting members, Figures 1.1(b) and 1.2. The purpose of this type of connection is to permit thermal induced movement of the panel relative to the supporting member. Thus, the only lateral restraint provided to the top chords of supporting trusses or joists is through friction in the clips and/or "drape" or "hugging" of the panels.

A comprehensive series of tests on standing seam roof systems supported by steel joists have been conducted at the Fears Structural Engineering Laboratory, University of Oklahoma[2]. The results of these tests indicate that (a) in certain cases, significant lateral restraint is provided by standing seam roof systems and (b) current specification rules are inadequate for design of top chords supporting standing seam panels. In the cited research, results from 46 full-scale tests using 40 ft., 50 ft. and 60 ft. span joists show that failure loads predicted using SJI design rules for joists supporting conventional roof decks, SJI design rules for unsupported top chords during construction and American Institute of Steel Construction specification[3] provisions for out-of-plane column buckling are inconsistent with the test results. For certain spans and joist types each of the methods were independently found to be either very conservative or unconservative. Thus, the current investigation was initiated with the objective of developing design procedures for the compression chords of light trusses or steel joists supporting standing seam roof decks. The study is limited to truss and joist configurations and member sizes similar to the SJI J- and H- series joists. However, both standard web types, "angle" and "rod" are considered. An "angle" web joist is constructed using equal leg angles crimped at top and bottom chord panel points and welded between the chord

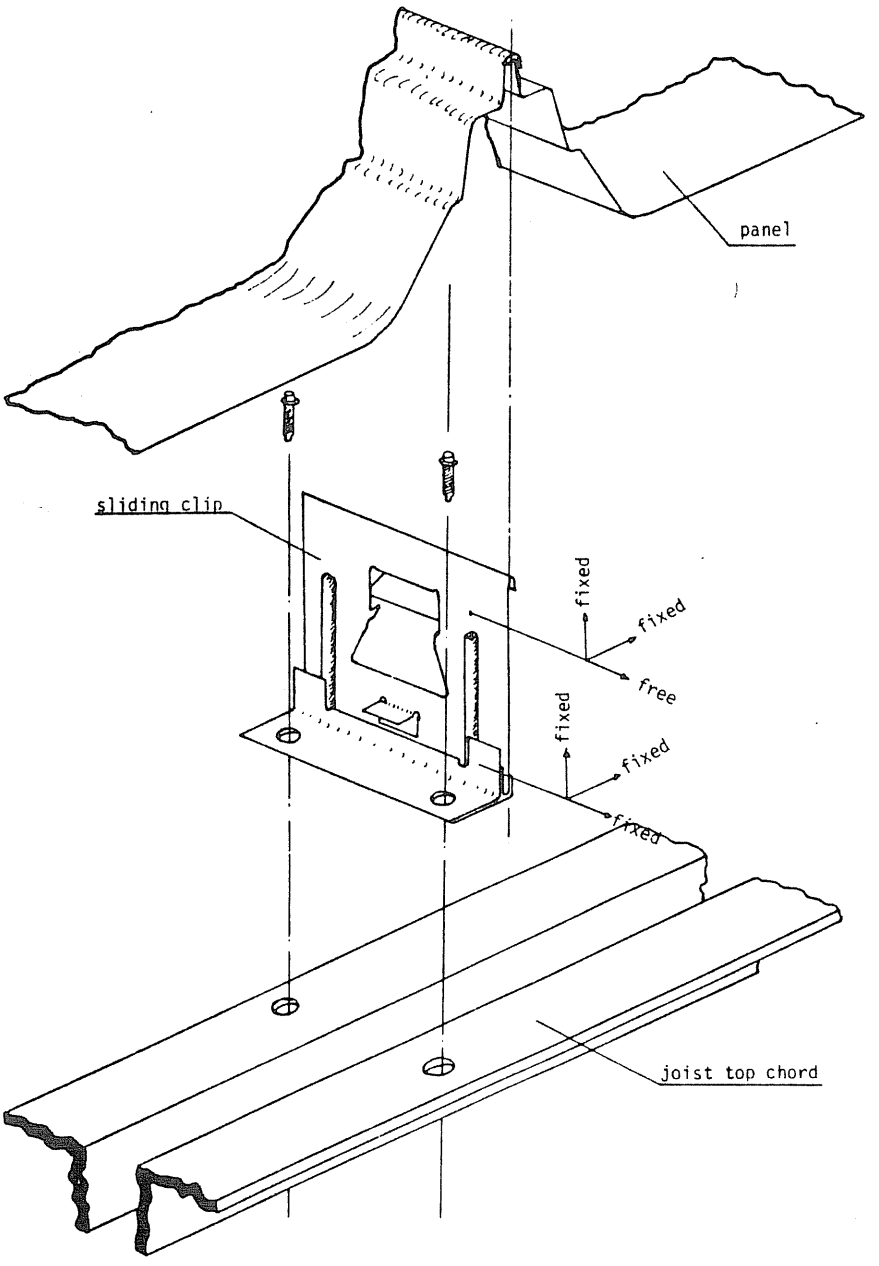


Figure 1.2 Standing Seam Roof Components

angles as shown in Figure 1.3(a). A "rod" web joist is constructed using a continuous round rod bend and welded to the top chord members as shown in Figure 1.3(b). The major difference between the two types is that angle web members are discontinuous, whereas the rod web members are made of one continuous rod.

## 1.2 Current Steel Joist Design Practices

The current SJI specification[1] has three provisions for the design of compression chords of J- and H- series joists. The first provision considers only column buckling in the plane of the web of the joist. Use of this provision is limited to situations where (a) each attachment of the supported slab or deck to the top chord is capable of resisting at least 300 lbs., (b) the spacing of the attachment is not greater than 36 in., and (c) the panel length (distance between attached web members) is less than 24 in. If these conditions are met, the allowable compression stress is determined from

$$F_a = \frac{\left[1 - \frac{(p/r)^2}{2\,C_c^2}\right] Q\, F_y}{\frac{5}{3} + \frac{3}{8}\left(\frac{p/r}{C_c}\right) - \frac{1}{8}\left(\frac{p/r}{C_c}\right)^3} \qquad \text{for } (p/r) \le C_c \qquad (1.1a)$$

Where $F_a$ = allowable chord stress, $C_c = \sqrt{2\pi^2 E/QF_y}$, Q is a form factor equal to unity unless the width-thickness ratio of one or more elements of the profile exceeds the limits specified in the AISC Specification Section 1.9 for hot rolled sections[3] and in the AISI Specification Section 3 for cold formed sections[4], p = distance between panel points for the chord members, r = least radius of gyration of the chord, E = elasticity

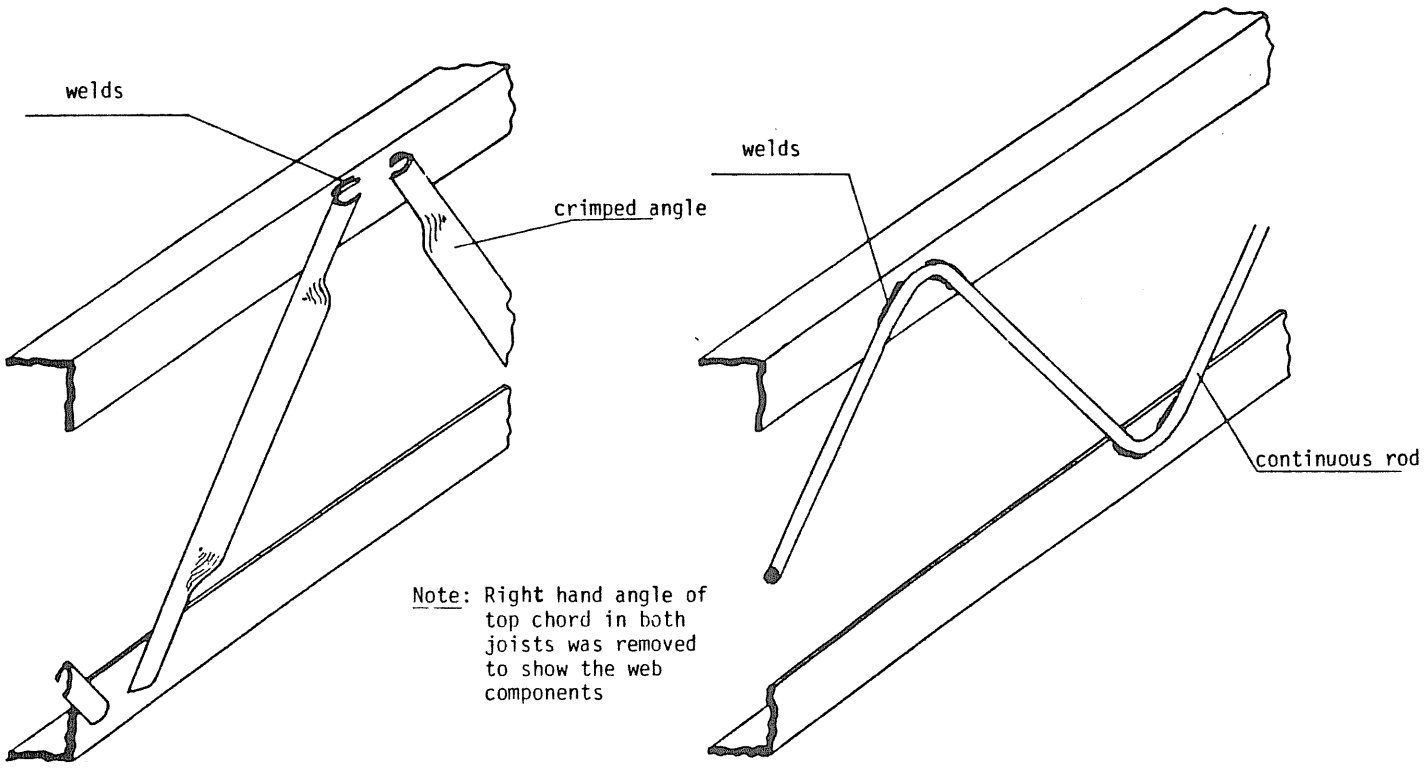


Figure 1.3 Angle and Rod Web Joists

modulus (usually taken equal to 29,000 ksi), or

$$F_a = \frac{12\ \pi^2\ E}{23\ (p/r)^2} \qquad \text{for } (p/r) > C_c \qquad (1.1b)$$

The factor of safety in Equation 1.1a is the denominator of that equation and ranges from 1.67 to 1.92 depending on the slenderness ratio; the factor of safety in Equation 1.1b is 23/12 (=1.92). Since the joist chord is considered to be laterally braced with respect to the vertical axis, the critical p/r ratio is about the horizontal axis $(p/r)_x$.

The above provision is identical to those found in the AISC specification for column buckling[3]. They were apparently adopted by SJI based on work conducted by Lenzen[5] as reported in Reference 6.

The second provision considered in-plane beam column effects. The above attachment provisions apply, but there is no limit on panel spacing. An adequate chord is one which satisfies (a) at the panel points

$$f_a + f_b \leq 0.6\ F_y \qquad (1.2a)$$

and (b) at mid-panel

$$\frac{f_a}{F_a} + \frac{C_m\ f_b}{(1 - \frac{f_a}{F'_e})QF_b} \leq 1.0 \qquad (1.2b)$$

Where $C_m = 1 - 0.3\ f_a/F'_e$ for end panels, or $C_m = 1 - 0.4\ f_a/F'_e$ for interior panels, $f_a$ = computed axial unit compressive stress, $f_b$ = computed bending unit compressive stress at the point under consideration, $F_a$ = allowable axial unit compressive stress based on p/r as defined previously, $F_b$= allowable bending unit stress, $F'_e = 12\ \pi^2\ E/23(p/r)^2$, Q is a

form factor defined previously. The factor of safety for equation 1.2a is at least 1.67. The factor of safety for Equation 1.2b can not be determined in general but is assumed to exceed 1.67. Again this provision is identical to those contained in the AISC specification for beam-columns except for the expressions for $C_m$.

The third provision is to be used to assess lateral stability of joists during erection. The SJI specification requires that the chord properties be such that $F_a \geq 10{,}000$ psi where

$$F_a = \frac{14.15 \times 10^6 C_1 C_2}{h\, S^2\, A_T} \sqrt{(I_T+I_B)(J_T+J_B)S^2+25.6\, I_T I_B\, h^2} \qquad (1.3)$$

In which S = bridging spacing (in.), h = effective joist depth (in.), $A_T$= area of top chord ($in.^2$), $I_T$= moment of inertia of top chord about the vertical axis ($in.^4$), $I_B$= moment of inertia of bottom chord about the vertical axis ($in.^4$), $J_T$= torsional constant of top chord, $J_B$= torsional constant of bottom chord, $J_T$ and $J_B$ are calculated from the formula $J = \Sigma\, At^2/3$, $C_1$= 0.85 for two-piece chord joist, or $C_1$= 1.00 for one-piece chord joist, $C_2$ is a constant with values listed in Table 1.1.

Table 1.1 Constant C2 values for Equation (1.3)

| Number of Rows of Bridging | $C_2$ |
|---|---|
| 1 | 4.00 |
| 2 | 3.00 |
| 3 | 4.00 |
| 4 | 3.33 |
| 5 | 4.00 |

Equation 1.3 is an empirical relationship based on the work of J. A. Hribar[6] and it takes into account possible lateral restraint supplied to the top chord from the web and bottom chord members due to

bending in these members during lateral movement of the top chord. The theoretical analysis used to develop Equation 1.3 is based on the conservation of energy principle. By assuming a buckled shape, a sinusoidal curve in this case, the strain energy due to deformation of the various joist components was calculated. The following were considered: (a) bending and twisting of the top and bottom chords, (b) bending and twisting of the web members, and (c) the work done by the external forces. On setting the strain energy equal to the work done, a value for the critical load was obtained. Due to the complicated geometry of joists, the resulting equations for strain energy and work done are extremely complex ( the strain energy equation had 53 terms all involving trigonometric functions of 2nd and 3rd orders ). Using the theoretical results, Hribar apparently developed Equation 1.3, however, literature concerning this development was not found. Tests confining the theoretical results are described in Reference 6.

The above provisions have been successfully used for the design of many thousands of steel joist supported roof systems that meet the specified limitations. However, unless the clip friction and/or restraint provided by panel drape or hugging provide sufficient lateral restraint, use of these provisions for standing seam roof systems may be unconservative. From the test results and comparisons to design predictions reported in Reference 2, it is apparent that sufficient restraint to allow the safe use of Equation 1.1 is not provided in a number of the configurations tested. Further, it was shown that Equation 1.3 did not accurately predict the failure loads when no lateral restraint was assumed; both conservative and unconservative results were obtained. Thus ,

it is apparent that further research is required to develop design methodology for light trusses and steel joists supporting standing seam roofs.

## 1.3 Scope of Current Research

A need to develop design procedure to accurately predict the load carrying capacity of steel joists and light trusses supporting standing seam roof systems has been shown. The research reported here is an attempt to satisfy this need. Chapter II summarizes the previous experimental program[2] which serves as the basis for comparison of the theoretical results developed in Chapter III. Two analysis procedures are developed. The first procedure is based on statics only. The second analysis procedure is based on existing iterative procedure to predict column (chord) buckling loads. Using results from the second analysis technique, a simplified design equation is developed in Chapter IV. These approximate results are then compared with the exact analysis results and with the experimental data available.

# CHAPTER II

# EXPERIMENTAL RESEARCH

## 2.1 Scope of Research

A research program to study the behavior of steel joists supporting standing seam roof system using simulated gravity loading was conducted at Fears Structural Engineering Laboratory, University of Oklahoma[2] and forms the basis for comparisons made in this study. This chapter is a detailed summary of the cited testing program and results. Analytical results developed in Chapter III are compared to the test results in Chapter IV. The primary purpose of this research was to determine lateral bracing spacing requirements for the joists, in addition to checking the adequacy of design procedures suggested by the Steel Joist Institute and the Americal Institute of Steel Construction for preventing out-of-plane lateral torsional instability of the top chord of steel joists when used with standing seam roof panels. The tests were designed and conducted to cover all parameters that were believed to affect the roof system. These parameters included joist span length, design live load level, bridging spacing, web type, insulation, clip size and roof insulation systems.

Three span lengths were used, 40, 50 and 60 ft. spans; two design load levels 20 and 40 psf; numerous bridging spacings; two web types, rod

and angle; two clip heights, 3 in. and 4 in.; and tests were conducted with and without insulation in place. In addition, a proprietory Roof Insulation System (RIS) was also installed in a few tests. Standard 1 in. bolted angle bridging was used in all tests. Bridging ranged from 1 to 11 rows of top chord bridging and from 3 to 12 rows of bottom chord bridging.

The following joist designation scheme was used throughout the project:

xx/y/zz-nn A

where xx = nominal span in ft., y = clip height in in., zz = nominal live load in psf, nn = test number in chronological order conducted, A = E for test joist on the east side of the test setup, = W for test joist on the west side of the test setup. For example, joist 40/3/20-14E refers to the east test joist in a 40 ft. span test with a 3 in. high clip and with 20 psf design live load and the test was the 14th test conducted in the series.

## 2.2 Overview of the Testing Procedure

For each test, the roof assembly was first constructed inside a 15 ft. 3 in. wide by 60 ft. 6 in. long vacuum chamber. Each test involved two test joists and two outside joists, all spaced at 4 ft. 9 in. on center. The four joists were suppoted by beams and short columns at each end of the vacuum chamber. Figure 2.1 depicts a completed test setup.

The outside joists were designed to have approximately 60% of the test joists flexural stiffness (moment of inertia) in order to prevent

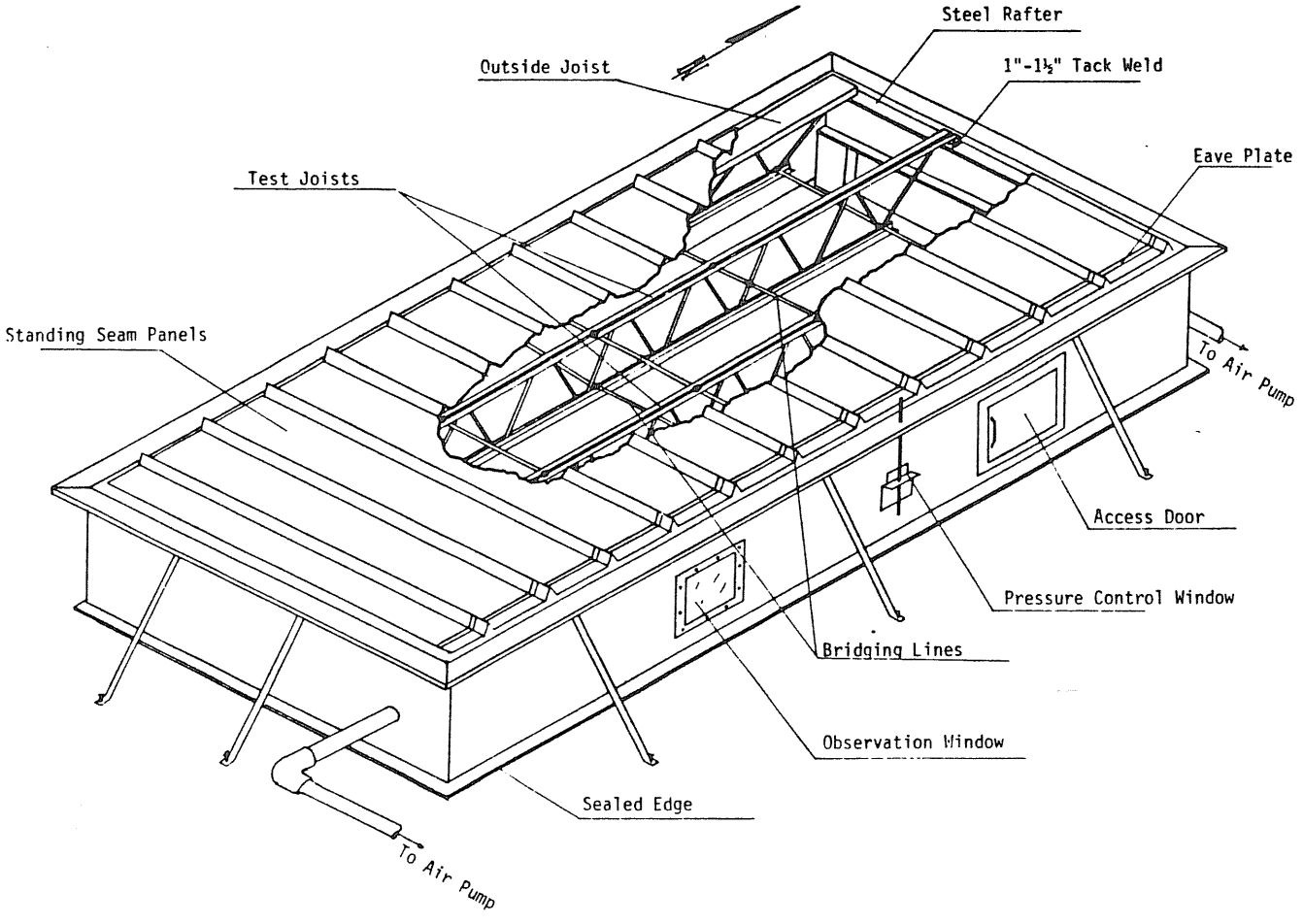


Figure 2.1 Simulated Gravity Loading Test Set-up

any flexural "bridging" of the standing seam panels. To simulate lateral restraint provided by an eave strut in a building installation, channel sections were welded to the top chord of the outside joists. Top chord bridging was attached to one channel in all tests (east side channel) and to both channels in some tests. Bottom chord bridging was installed near the outside bottom chord joist panel points in all tests with additional intermediate rows in some tests.

Simulated live load was applied using suction provided by three vacuum pumps installed and connected to the chamber walls. The air pressure was monitored using a standard U-tube monometer and an electronic pressure transducer. Vertical and lateral displacements were measured at predefined discrete points along the test and outside joists using linear displacement transducers. All data was read and recorded using a micro-computer based data acquisition system in "real time". Selected data was plotted as the test was being conducted.

Two series of supplementary tests were conducted as part of the research program. A test setup was constructed to measure lateral restraint provided by various clip/insulation combinations under simulated live load, see Figure 2.2. In addition, tension tests of chord angles were conducted to determine yield stress and elongation of the top chord material. The minimum specified yield stress of the joists, bridging angles and panels was 50,000 psi.

## 2.3 Construction Procedure Used for the Test Setups

### 2.3.1 Simulated Gravity Load Test Setup

The construction of all simulated gravity load test setups

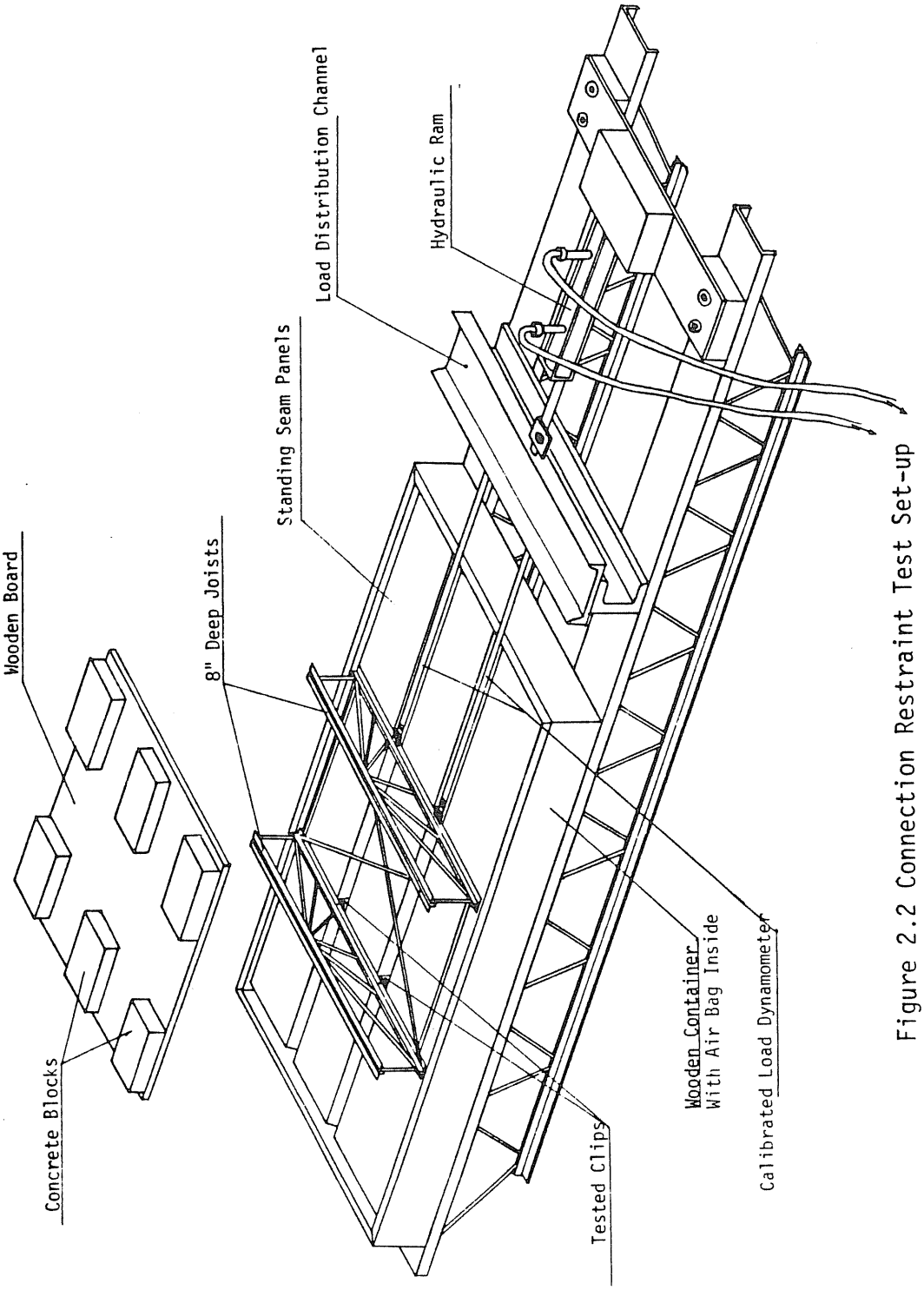


Figure 2.2 Connection Restraint Test Set-up

followed the procedure summarized in the following steps:

1) Test and outside joists were chosen and placed inside the chamber and spaced at 4 ft. 9 in. on center.

2) All joists were connected to rafter sections using 1½ to 2 in. long tack welds (see Figure 2.1).

3) The designated bridging configuration was installed. The bridging was bolted together and to the joist using 3/8 in. diameter, 3 in. long bolts and were tightened with an impact wrench.

4) The floating panel clips and the standing seam panels were installed at 2 ft. 0 in. spacing. If required, the insulation was installed along with the panels. In the case of RIS construction, the segmented beams were first installed on all four joists followed by the clips and panels.

5) The east end of the roof panels were fastened either directly to the channel on the east joist or to the eave closure plates previously installed on the channel or to RIS segmented beams, as previously explained.

6) The entire assembly was covered with 6 mil polythelene and sealed with vinyl tape.

7) Displacement transducers were installed in the designated locations using the access door in the chamber wall.

Once the assembly was completed and sealed, suction was applied using a vacuum pump and two auxiliary 55 gallon drum type industrial vacuum cleaners.

At the beginning of each test, a suction load of approximately 25% of the estimated failure load was first applied to the roof system.

Readings were taken and plotted to check the roof behavior and the data acquisition system operation. If any unreasonable results were observed at this time, the test was stopped and the problem was located and corrected properly. If no unreasonable results were detected, the system was unloaded and initial "zero" readings were taken. The suction load was then started and increased in preassigned increments depending on the joist design live load (25 plf for a 20 psf roof system and 50 plf for a 40 psf roof system ). This process was continued until approximately 1.5 times the service load was reached then the load increments were decreased to 5 plf until failure. Readings of all displacement transducers and the electronic monometer were taken at each load increments to monitor roof and joist behavior and failure modes.

2.3.2 Supplementary Tests

Connection Restraint Tests. Floating panel clips were first bolted to two short sections of 8 in. deep joists and the insulation, if used, and panels installed using the usual procedure. The assembly was then turned over and placed on the air bag in the containment box (see Figure 2.2). A hydraulic ram was then connected to the support framing using a linkage containing a calibrated load cell.

To perform a test, concrete blocks were first placed on the support frame. Air was then pumped into the air bag until the support frame was free of the containment box and the weight of the blocks was balanced by the pressure in the air bag. Using the hydraulic ram, force was then applied transverse to the panel. The displacement transducers were used to measure the motion of the support frame relative to the panel. The load cell was used to measure the applied force. The force and dis-

placement were measured and plotted in real time using the data acquisition system.

Coupon Tests. A 24 in. long section of the top chord in each tested joist was cut upon test completion and tested using a specially designed device mounted in a universal testing machine. The reported yield stress and tensile strength from these tests are found in section 2.4.3.

## 2.4 Test Results

### 2.4.1 Simulated Gravity Loading Test Results

Forty-six simulated gravity loading tests were performed. These tests included eighteen 40 ft. span, seven 50 ft. span and twenty-one 60 ft. span tests. Top chord lateral buckling was the failure mode for all tests with four exceptions. The failure modes for these four tests were reported to be due to the test setup, inadequacy of the outside joists or support failures. Data from these tests will not be included in the comparisons made in Chapter IV.

Comparison of experimental failure loads with allowable working loads obtained from each of the current analysis procedures "AISC", "SJI" and "CONV" were made and the results are reported here. The terms "SJI", "CONV" and "AISC" were used to identify the results. "CONV" refers to the SJI analysis procedure for chords braced by conventional decks as was described in Section 1.2. The associated failure mode is in-plane buckling of the compression chord. The factor of safety in this case is either the denominator in Equation 1.1a or 23/12 as in Equation 1.1b, whichever applies. "SJI" refers to the SJI analysis procedure for

erection stability as described in Section 1.2. The associated failure mode is lateral-torsional buckling of the joist top chord and web. The factor of safety is 2.0[7]. "AISC" refers to the analysis procedure for unbraced compression chords without considering the effect of the web as described in Section 1.2. The associated failure mode is lateral buckling of the top chord. The factor of safety is the same as given in the "CONV" design procedure. The allowable working loads for each joist were calculated using the measured yield stress of the compression chord material. The comparisons were based on a load factor (LF) defined as:

$$LF = \frac{\text{Experimental Failure Load}}{\text{(Predicted Failure Load/Factor of Safety)}} \qquad (2.1)$$

40 ft. Span Tests. Eighteen tests using 40 ft. span angle and rod web joists were reported. Design load levels of 20 psf and 40 psf and 5 ft. joist spacing were used to develop the test matrix. Three bridging spacing configurations were used for top and bottom chords. Bottom chord bridging was installed near the outside bottom chord panel point and at midspan for all tests. A flow chart of the test matrix is shown in Figure 2.3. Experimental failure loads, allowable loads from "AISC", "SJI", and "CONV" analyses and associated load factors are given in Table 2.1 (from Reference 2).

50 ft. Span Tests. Seven tests using 50 ft. span angle joists were reported. Design load level of 40 psf and 5 ft. joist spacing were used to develop the test matrix. Four bridging spacing configurations were used for top and bottom chords. Bottom chord bridging was installed near the outside bottom chord panel points for all tests. Four

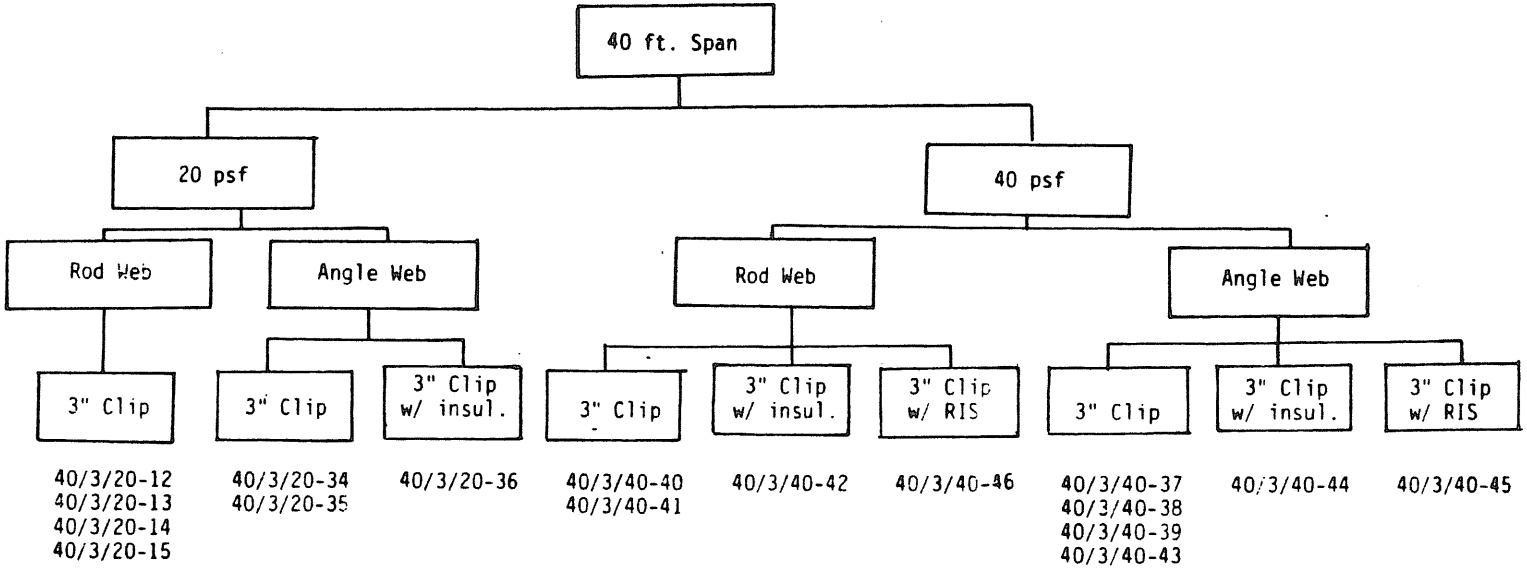


Figure 2.3 40 ft. Span Tests Flow Chart
(from Reference 2)

Table 2.1
40 ft. Span Test Results (from Reference 2)

| | | Test No. | Rows of Bridg. T | Rows of Bridg. B | Exp. $w_E$ (plf) | y-Axis (AISC) w plf | y-Axis (AISC) LF | Bridging (SJI) w plf | Bridging (SJI) LF | x-Axis (CONV.) w plf | x-Axis (CONV.) LF | Insulation |
|---|---|---|---|---|---|---|---|---|---|---|---|---|
| 20 psf | Rod | 40/3/20-12 | 1 | 3 | 208.7 | 10.5 | 19.97 | 18.2 | 11.48 | 130.5 | 1.60 | N |
| | | 40/3/20-13 | 3 | 3 | 278.1 | 42.8 | 6.5 | 65.2 | 4.27 | 131.9 | 2.11 | N |
| | | 40/3/20-14 | 3 | 3 | 238.2 | 45.4 | 5.25 | 65.1 | 3.66 | 126.2 | 1.89 | N |
| | | 40/3/20-15 | 3 | 3 | 268.0 | 39.7 | 6.76 | 65.9 | 4.07 | 117.7 | 2.28 | N |
| | Angle | 40/3/20-34[1] | 3 | 3 | 284.9 | | | | | | | N |
| | | 40/3/20-35 | 3 | 3 | 235.9 | 58.0 | 4.07 | 84.9 | 2.78 | 130.0 | 1.81 | N |
| | | 40/3/20-36 | 3 | 3 | 254.5 | 61.0 | 4.17 | 95.9 | 2.65 | 136.1 | 1.87 | I |
| 40 psf | Rod | 40/3/40-40 | 3 | 3 | 421.2 | 86.2 | 4.89 | 150.0 | 2.81 | 232.1 | 1.81 | N |
| | | 40/3/40-41 | 3 | 3 | 418.1 | 85.5 | 4.89 | 145.8 | 2.87 | 221.3 | 1.89 | N |
| | | 40/3/40-42 | 3 | 3 | 433.5 | 86.2 | 5.03 | 144.5 | 3.00 | 228.2 | 1.90 | I |
| | | 40/3/40-45 | 3 | 3 | 340.9 | 84.8 | 4.02 | 149.9 | 2.27 | 222.2 | 1.53 | R |
| | Angle | 40/3/40-37[1] | 3 | 3 | 302.2 | | | | | | | N |
| | | 40/3/40-38[1] | 3 | 3 | 417.2 | | | | | | | N |
| | | 40/3/40-39 | 3 | 3 | 385.9 | 124.4 | 3.10 | 193.2 | 2.00 | 222.4 | 1.74 | N |
| | | 40/3/40-43 | 3 | 3 | 382.4 | 119.0 | 3.21 | 190.8 | 2.00 | 227.5 | 1.68 | N |
| | | 40/3/40-44 | 3 | 3 | 376.3 | 128.9 | 2.92 | 197.6 | 1.90 | 226.8 | 1.66 | I |
| | | 40/3/40-46 | 3 | 3 | 347.3 | 115.6 | 3.00 | 188.9 | 1.84 | 230.5 | 1.51 | R |
| * | | 40/3/20-11 | 1 | 3 | 314.2 | 12.8 | 24.48 | 22.1 | 14.21 | 169.8 | 1.85 | |

*Retest of Test B-2B of Reference 5.

[1]Test not considered to be valid.

N = w/o insulation

I = w/ insulation

R = RIS Beams

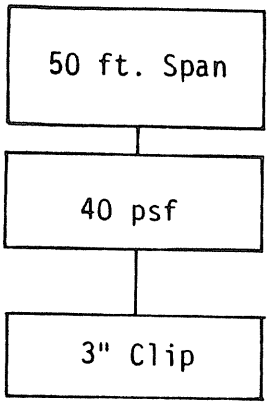


50/3/40-27
50/3/40-28
50/3/40-29
50/3/40-30
50/3/40-31
50/3/40-32
50/3/40-33

Figure 2.4 50 ft. Span Tests Flow Chart
(from Reference 2)

Table 2.2
50 ft. Span Test Results (from Reference 2)

| | Test No. | Rows of Bridg. T | Rows of Bridg. B | Exp. $w_E$ (plf) | y-Axis (AISC) w plf | y-Axis (AISC) LF | Bridging (SJI) w plf | Bridging (SJI) LF | x-Axis (CONV.) w plf | x-Axis (CONV.) LF |
|---|---|---|---|---|---|---|---|---|---|---|
| Angle Web | 50/3/40-31 | 3 | 7 | 264.1 | 123.2 | 2.14 | 202.8 | 1.30 | 224.6 | 1.18 |
| | 50/3/40-33 | 3 | 7 | 367.7 | 123.0 | 2.99 | 197.3 | 1.86 | 222.2 | 1.65 |
| | 50/3/40-29 | 5 | 7 | 422.2 | 191.7 | 2.20 | 282.1 | 1.50 | 223.6 | 1.89 |
| | 50/3/40-30 | 5 | 7 | 347.6* | 189.5 | | 281.4 | | 224.6 | |
| | 50/3/40-32 | 5 | 7 | 349.3 | 187.8 | 1.86 | 274.2 | 1.27 | 222.2 | 1.57 |
| | 50/3/40-28 | 6 | 7 | 334.3* | 207.4 | | 282.1 | | 223.6 | |
| | 50/3/40-27 | 7 | 7 | 334.2* | 215.4 | | 282.1 | | 223.6 | |

*Not conducted to failure.
All tests conducted without insulation.

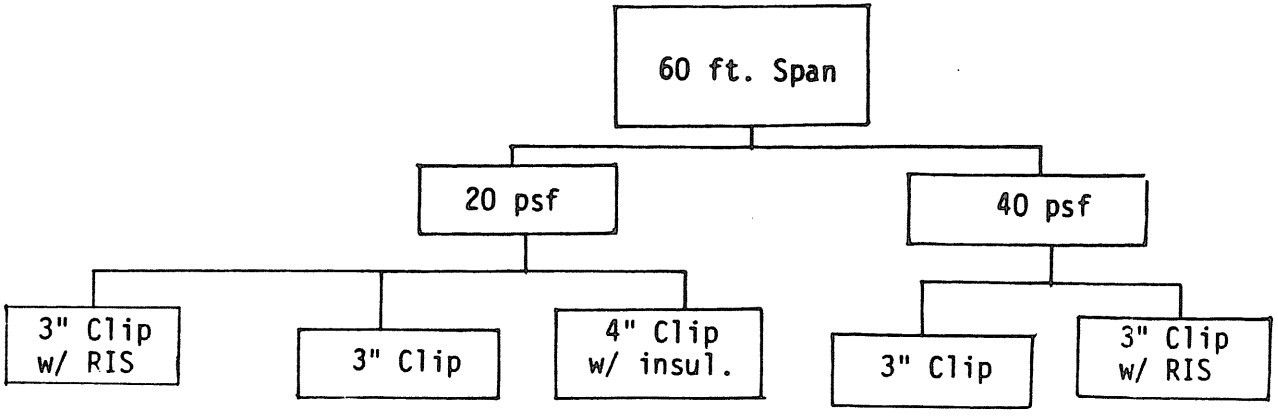


60/3/20-26

60/3/20-3
60/3/20-4
60/3/20-5
60/3/20-6
60/3/20-7
60/3/20-8
60/3/20-9
60/3/20-16
60/3/20-17
60/3/20-18
60/3/20-19
60/3/20-20
60/3/20-21
60/3/20-26

60/4/20-1
60/4/20-2

60/3/40-10
60/3/40-22
60/3/40-23

60/3/40-24
60/3/40-25

Figure 2.5 60 ft. Span Tests Flow Chart
(from Reference 2)

Table 2.3
60 ft. Span Test Results (from Reference 2)

| | | Test No. | Rows of Bridg. T | Rows of Bridg. B | Exp. $w_E$ (plf) | y-Axis (AISC) w plf | y-Axis (AISC) LF | Bridging (SJI) w plf | Bridging (SJI) LF | x-Axis (CONV.) w plf | x-Axis (CONV.) LF | Insulation |
|---|---|---|---|---|---|---|---|---|---|---|---|---|
| Angle Web | 20 psf | 60/3/20-4 | 1 | 3 | 110.0 | 5.1 | 21.43 | 11.5 | 9.55 | 130.6 | 0.84 | N |
| | | 60/3/20-1 | 2 | 4 | 111.7 | 12.5 | 8.95 | 18.6 | 5.90 | 120.3 | 0.93 | I* |
| | | 60/3/20-2 | 2 | 4 | 111.7 | 11.6 | 9.65 | 18.3 | 6.11 | 127.0 | 0.88 | I* |
| | | 60/3/20-5 | 3 | 5 | 162.9 | 22.7 | 7.16 | 40.2 | 4.05 | 123.6 | 1.32 | N |
| | | 60/3/20-6 | 3 | 5 | 170.5 | 30.2 | 5.64 | 56.6 | 3.01 | 123.9 | 1.38 | N |
| | | 60/3/20-3 | 4 | 6 | 123.0 | 25.5 | 4.86 | 49.0 | 2.52 | 120 | 1.03 | N |
| | | 60/3/20-7 | 5 | 7 | 197.8 | 54.6 | 3.62 | 81.7 | 2.42 | 126.0 | 1.57 | N |
| | | 60/3/20-8 | 5 | 7 | 138.4 | 52.9 | 2.62 | 82.3 | 1.68 | 128.6 | 1.08 | N |
| | | 60/3/20-9 | 5 | 7 | 128.9 | 55.1 | 2.34 | 91.5 | 1.41 | 129.8 | 0.99 | N |
| | | 60/3/20-16 | 5 | 7 | 133.5 | 52.4 | 2.55 | 81.1 | 1.65 | 121.4 | 1.10 | N |
| | | 60/3/20-17 | 5 | 7 | 210.4 | 82.7 | 2.43 | 128.6 | 1.57 | 121.7 | 1.66 | N |
| | | 60/3/20-18 | 5 | 7 | 148.3 | 83.3 | 1.78 | 128.6 | 1.15 | 123.8 | 1.20 | N |
| | | 60/3/20-26 | 5 | 7 | 153.2 | 81.5 | 1.88 | 129.7 | 1.18 | 123.4 | 1.24 | N |
| | | 60/3/20-19 | 6 | 8 | 163.1 | 102.0 | 1.60 | 156.7 | 1.04 | 124.7 | 1.31 | N |
| | | 60/3/20-20 | 10 | 12 | 180.4 | 122.9 | 1.47 | 151.3 | 1.19 | 119.4 | 1.51 | N |
| | | 60/3/20-21 | 10 | 12 | 187.8 | 122.5 | 1.53 | 150.9 | 1.24 | 120.0 | 1.57 | N |
| | 40 psf | 60/3/40-10 | 5 | 7 | 316.5 | 121.3 | 2.61 | 174.1 | 1.82 | 214.0 | 1.48 | N |
| | | 60/3/40-24 | 5 | 7 | 306.6 | 162.4 | 1.89 | 241.8 | 1.27 | 209.9 | 1.46 | R |
| | | 60/3/40-25 | 5 | 7 | 309.1 | 163.5 | 1.89 | 244.3 | 1.27 | 211.9 | 1.46 | R |
| | | 60/3/40-23 | 10 | 7 | 399.3 | 209.4 | 1.91 | 241.2 | 1.66 | 209.5 | 1.91 | N |
| | | 60/3/40-22 | 11 | 7 | 411.8 | 209.4 | 1.97 | 241.2 | 1.71 | 209.5 | 1.97 | N |

*4 in. clips w/ insulation and thermal blocks.
N = w/o Insulation.
I = w/ 4 in. clip, insulation and thermal blocks.
R = RIS Beams

of the seven tests were conducted to failure. Tests 27, 28 and 29 were conducted using the same joists but with different bridging spacing. First Test 27 was conducted to a predetermined load level and then unloaded. The number of rows of bridging was then changed from seven to six and Test 28 was conducted to a higher predetermined load and then unloaded. The number of rows of bridging was then changed from six to five and Test 29 was conducted to failure. The same procedure was used for Tests 30 and 31 with five and three rows of bridging, respectively. Tests 32 and 33 were conducted directly to failure. A flow chart of the test matrix is shown in Figure 2.4. Experimental failure loads, allowable loads from "AISC", "SJI" and "CONV" analyses and associated load factors are given in Table 2.2 (from Reference 2).

60 ft. Span Tests. Twenty-one tests using 60 ft. span angle web joists were reported. Design load levels of 20 and 40 psf and 5 ft. joist spacing were used to develop the test matrix. Seven bridging spacing configurations were used for top and bottom chords. Bottom chord bridging was installed near the outside bottom chord panel points for all tests. A flow chart of the test matrix is shown in Figure 2.5. Experimental failure loads, allowable loads from "AISC", "SJI" and "CONV" analyses and associated load factors are given in Table 2.3 (from Reference 2).

### 2.4.2 Connection Restraint Test Results

Using the test setup described in Section 2.3.2, one hundred and six connection restraint tests were conducted by Holland and Murray[2] using the standing seam roof system. Thirty-eight tests were performed using a 4 in. clip with insulation and thermal blocks, forty-two tests

with a 3 in. clip and insulation and twenty-six tests with a 3 in. clip and no insulation. The tests were conducted at five load levels, representing 12, 20, 40, 55 and 70 psf. The effective coefficient of friction is defined as

$$CF = \frac{\text{Lateral Force Required to Produce Slip Per Clip}}{\text{Normal Force Per Clip}} \qquad (2.2)$$

Table 2.4 summarizes the test results showing the average friction force (FF) and the average effective coefficient of friction (CF) for each connection configuration at each load level along with the corresponding standard deviation. Data from Table 2.4 is shown plotted in Figures 2.6 and 2.7 as friction force versus normal force and effective coefficient of friction versus normal force, respectively. It is seen from those figures that the friction force increases relatively linearly with increasing normal force and that the effective coefficient of friction generally decreases with increasing normal force, but tends to level off above 40 psf.

Best fit polynomial function curves for each of the connection configurations are as follows:

4-in. clip with insulation and thermal block

$$FF = 58.04 + 0.04436\ (NF) + 3.038 \times 10^{-4}(NF)^2 \qquad (2.3)$$

3-in. clip with insulation

$$FF = 44.92 + 0.1985\ (NF) + 5.058 \times 10^{-5}(NF)^2 \qquad (2.4)$$

3-in. clip without insulation

$$FF = 38.91 + 0.2454\ (NF) - 4.396 \times 10^{-4}(NF)^2 \qquad (2.5)$$

These equations are limited to a normal force range of 120 lbs. to 700 lbs. per clip.

Table 2.4
Results of Connection Test for VULCRAFT
Standing Seam Roof Clips

(from Reference 2)

| | | 4" Clip w/insul. | | 3" w/ insul. | | 3" w/o insul. | |
|---|---|---|---|---|---|---|---|
| | | $\bar{X}$ | S | $\bar{X}$ | S | $\bar{X}$ | S |
| 120 psf | FF | 67.3 | 5.32 | 69.2 | 3.87 | 68.4 | 9.02 |
| | CF | 0.5599 | 0.0435 | 0.5371 | 0.0909 | 0.5681 | 0.076 |
| 200 psf | FF | 79.8 | 5.6789 | 86.7 | 14.2 | 86.8 | 6.11 |
| | CF | 0.399 | 0.0287 | 0.4333 | 0.0703 | 0.4333 | 0.031 |
| 400 psf | FF | 124 | 6.5574 | 133.7 | 19.4 | 139.7 | 16.3 |
| | CF | 0.3099 | 0.0166 | 0.3343 | 0.0483 | 0.3493 | 0.0408 |
| 550 psf | FF | 174.4 | 22.48 | 167.7 | 12.8 | 168.8 | 3.70 |
| | CF | 0.3171 | 0.0406 | 0.3048 | 0.023 | 0.3063 | 0.0068 |
| 700 psf | FF | 238 | 21.86 | 209.3 | 6.9 | 209.8 | 9.23 |
| | CF | 0.3398 | 0.0313 | 0.2989 | 0.0105 | 0.2995 | 0.0132 |

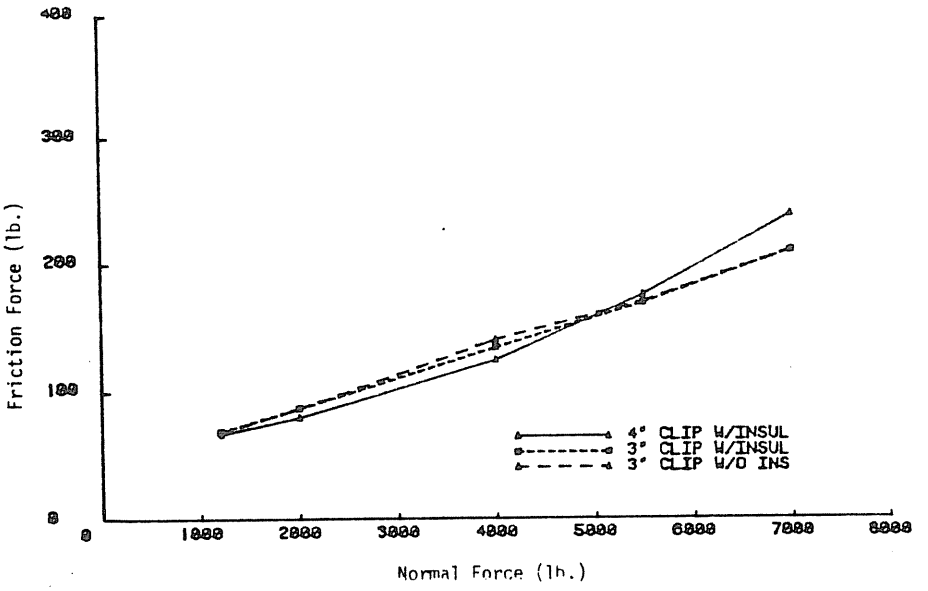


Figure 2.6 Friction Force vs. Normal Force

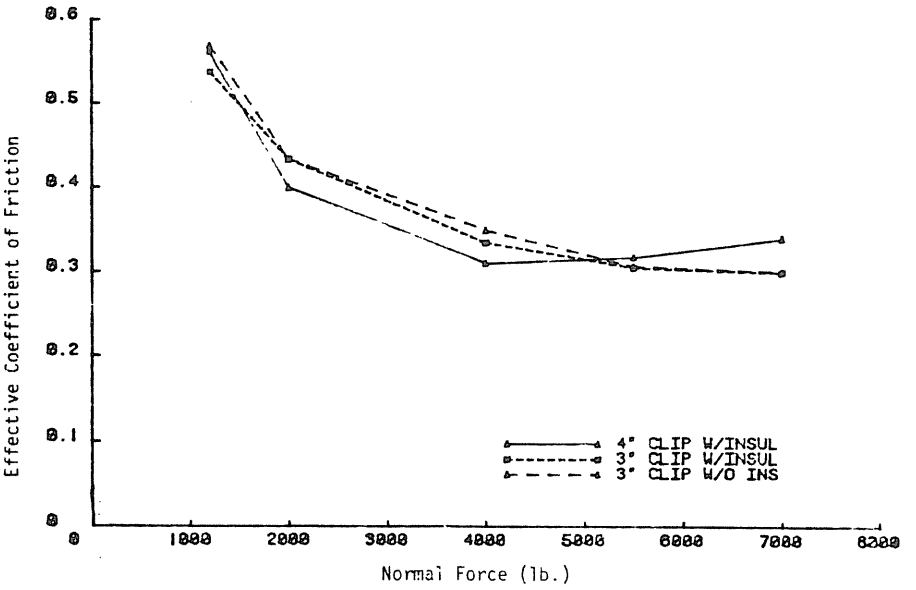


Figure 2.7 Effective Coeffecient of Friction vs. Normal Force

2.4.3. Coupon Test Results

A 24 in. long section of the top chord in each failed joist was cut after test completion and tested. A total of one hundred and five samples were made and tested. The average yield stress for all tests was 53.0 ksi. The yield stress values ranged from 46.7 to 61.0 ksi., whereas the tensile strength values ranged from 52.9 to 88.9 ksi. Percent elongation ranged from 2.2% to 29.1%. The standard deviation of the yield stress values was 2.92.

## 2.5 Conclusion From Experimental Data

The results shown in Tables 2.1, 2.2 and 2.3 include the load factors associated with the current three design procedures, as was explained in Section 1.2, for 40, 50 and 60 ft. span joists. These results were either conservative or unconservative depending on midspan bridging spacing and the procedure used. A conservative load factor is defined here as one that exceeds 1.67, 2.0 and 1.67 for "AISC", "SJI" and "CONV" procedures respectively; whereas an unconservative load factor is one that falls short of these numbers.

"AISC" Procedure. The load factors associated with this procedure were very conservative for large midspan bridging spacing but reasonable for small midspan bridging spacing. The load factors ranged from 21.43 for 30 ft. bridging spacing to 1.48 for 4 ft. bridging spacing.

"SJI" Procedure. The load factors associated with this procedure were conservative for large midspan bridging spacing and unconservative for small spacing. The load factors ranged from 11.48 for

20 ft. midspan bridging spacing to 1.04 for 4 ft. spacing. This procedure uses an empirical equation that was developed based on experimental research and for equal bridging spacing. It was used here for both equal and unequal bridging spacings.

"CONV" Procedure. The load factors associated with this procedure were unconservative for large midspan bridging spacings and reasonable for small spacings. The load factors ranged from 0.84 for 30 ft. spacing to 1.97 for 4 ft. spacing.

Based on the data discussed here, it is shown that none of the current design procedures reviewed is sufficiently accurate for buckling load prediction for joists supporting standing seam roof systems. The current theoretical research will study the disadvantages of the current design formulas and try to develop a new method that better studies light trusses and open web steel joists in conjunction with the standing seam roof systems.

# CHAPTER III

# THEORETICAL STUDY

## 3.1 Discussion

Test results reviewed in the previous chapter indicate that the three available design procedures are inadequate to evaluate the load carrying capacity of steel joists and light trusses supporting standing seam roof systems. Two possible explanations are: (1) The restraint provided by clip friction or panel "hugging" is neglected or (2) restraining effect of the web members is either neglected or inaccurately evaluated. Two analyses procedures are developed in this chapter which account for the above phenomena.

The standing seam roof system consists of panels and clips. The main purpose of the clip is to transfer normal load on the panels to the joists. The clips are restrained from moving in the joist longitudinal direction and free in the transverse direction, see Figure 1.2. Impending longitudinal motion of the lower section of the clip is resisted by friction forces in the sliding mechanism. In addition, because of the flexibility of the "pan" portion of the roof panel, the panel tends to "drape" on the top chord of the supporting truss or joist. Both effects tend to resist transverse motion of the top chord of the supporting member. Deter-

mination of these restraining effects on the load carrying capacity of the supporting member is the objective of the first analytical method, Section 3.2.

Lateral movement of the top chord causes bending of the web members and associated top chord restraint. This restraint is accounted for in the "SJI" design rules for construction, Equation 1.3. However, its application is limited to equal bridging spacing and assumes that the maximum chord force between bridging lines exists along the entire chord length. This assumption is conservative and may be satisfactory for closely spaced bridging lines, however, sharp reduction in chord force occurs over relatively short distances along the chord, see Figures 3.1 and 3.2. Due to this axial load reduction, the buckling load is higher than it is for the same chord with constant axial force. Web restraint effects and the variation in axial force in chord members between points of lateral restraint are included in the analytical method developed in Section 3.3.

## 3.2 Clip-Frictional Force Effect Method

### 3.2.1 Discussion

It is desired that the effect on load carrying capacity of restraining forces provided by a standing seam roof system be determined. A simplified model will be developed herein to represent the top chord and roof clips. The following assumptions are made in the analysis:

1) The top chord of an open web steel joist is represented by a column with one axial load acting at its end.

2) The column length is taken equal to the top chord bridging spacing S.

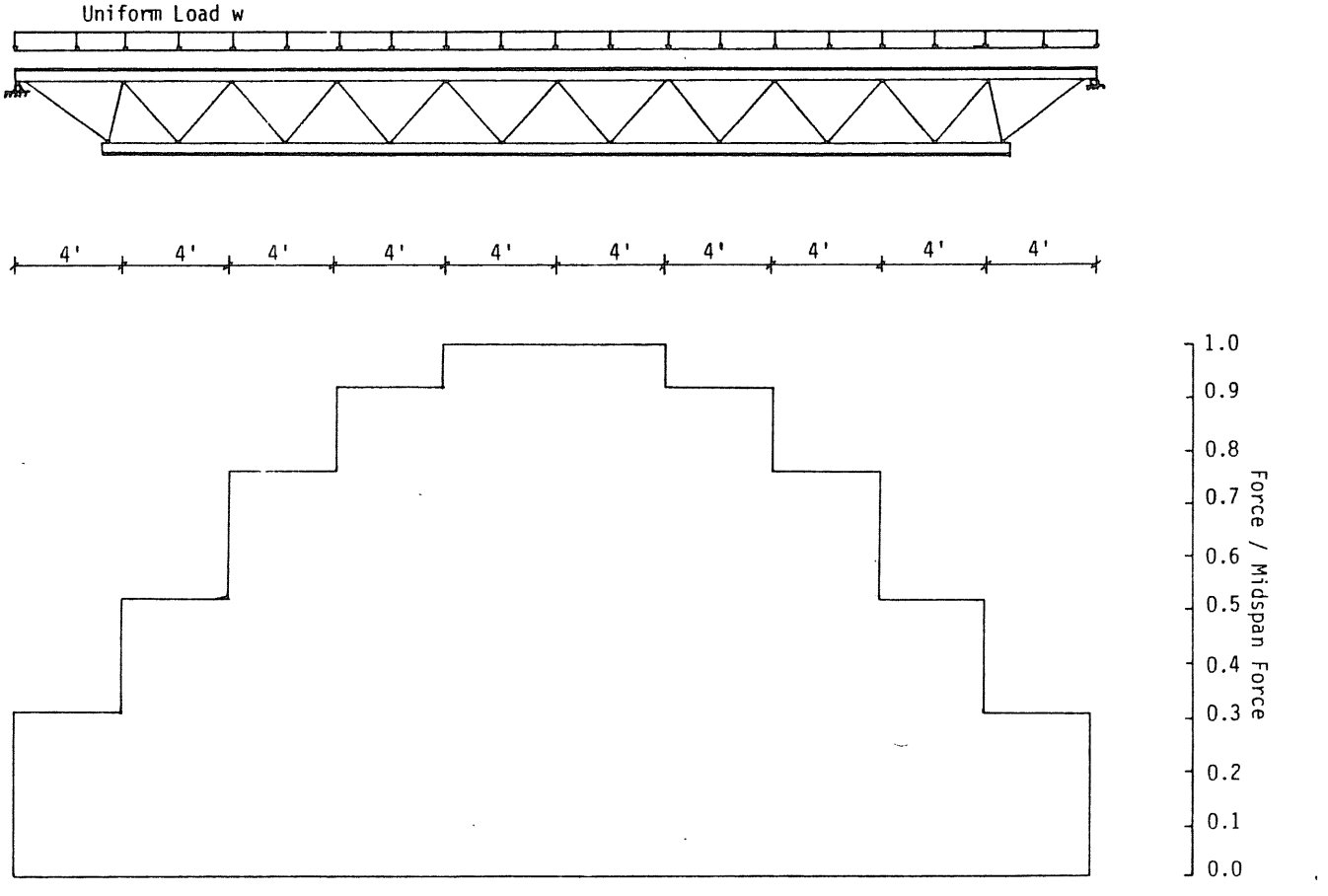


Figure 3.1 Variation of Axial Force Along the Top Chord for 40 ft, Span Angle Web Joist

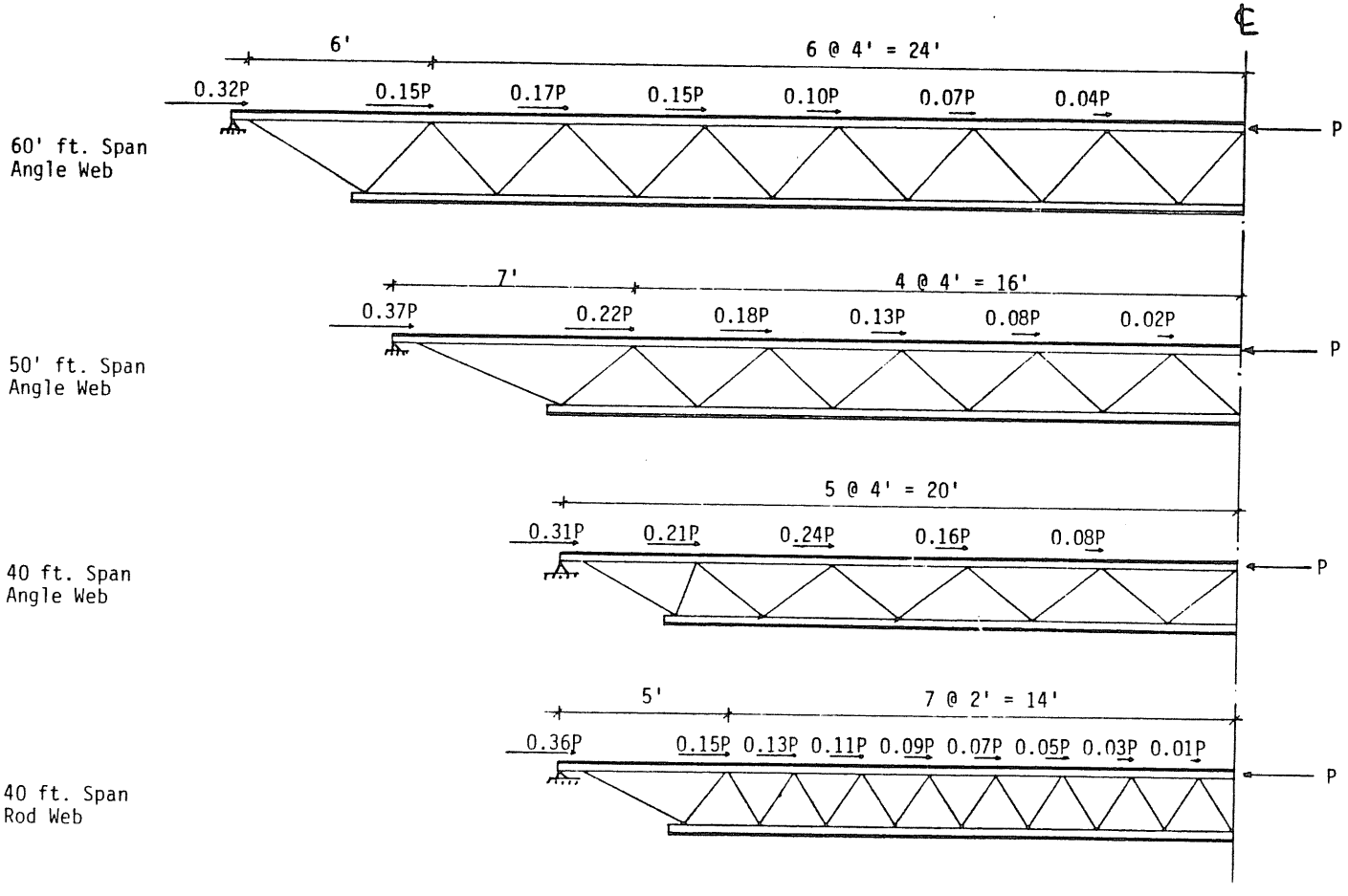


Figure 3.2 Chord Force Distribution for Joists Tested at Fears Laboratory

3) The effective column length factor k is taken, conservatively, equal to 1.0.

4) The web effect is neglected.

5) The governing buckling mode is a sinusoidal curve.

6) Buckling occurs in the horizontal plane, out-of-plane.

Making use of these assumptions, the top chord is represented by a pin-pin column as shown in Figure 3.3a. The forces, (FF), represent the combined clip friction and panel "hugging" forces and are assumed to be concentrated at the clip location. The clip forces are absent if the top chord force is below the buckling load. When the load P reaches the column buckling load, $P_{cr}$, the column tries to move laterally but is restrained by the forces FF. When the load P reaches a value where the clips can no longer restrain the column failure occurs, see Figure 3.3b. The value of maximum friction forces (FF) provided by the clips is determined from Equations 2.3 through 2.5 for different clip configurations.

3.2.2 Method Development

It is assumed the normal force transferred from the roof panel to the joist top chord through each clip is equal to the total uniform force applied on one panel. Making use of that assumption gives:

$$NF = w\ s' \tag{3.1}$$

where NF = normal force, w = normal uniform load on the joist, and s' = spacing of clips or panel width. The maximum joist bending moment is

$$M_{max} = w\ L^2/8 \tag{3.2}$$

where $M_{max}$ = bending moment at midspan, and L = joist span. Substituting Equation 3.1 into Equation 3.2 gives

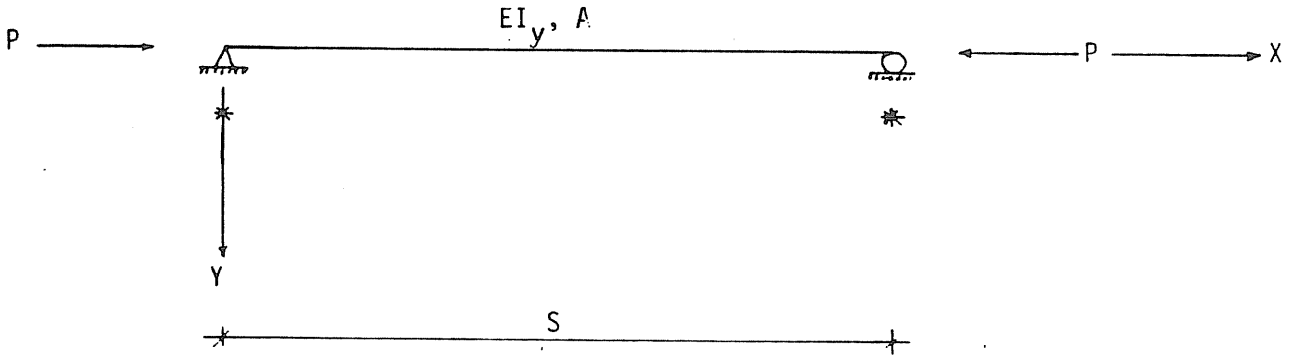


(a) Before Buckling

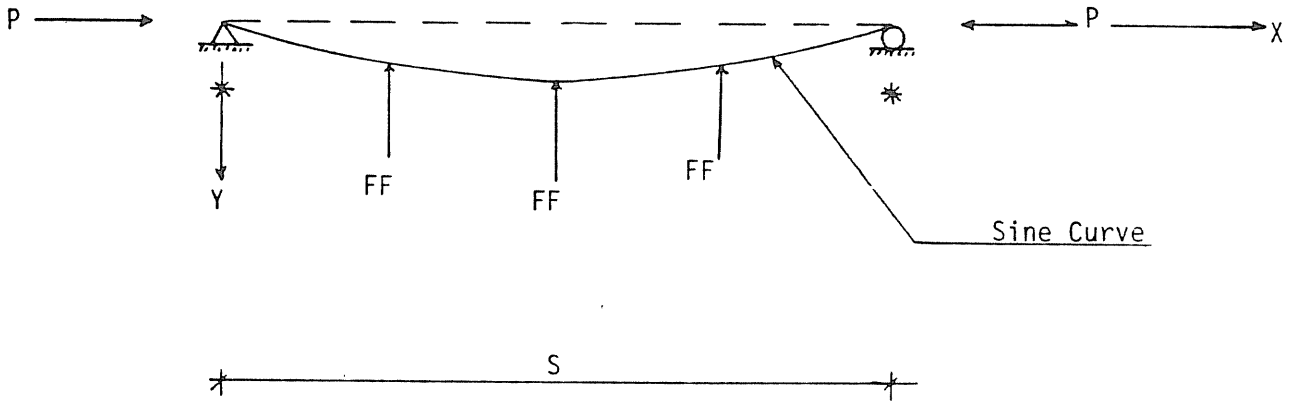


(b) After Buckling

* Bridging Line Location

Figure 3.3 Assumed Deflected Shape of Top Chord Between Bridging Lines

$$M_{max} = (NF)L^2 / 8\ s' \tag{3.3}$$

The maximum chord force can be estimated from

$$P = M_{max}/d \tag{3.4}$$

where P = axial force acting on top or bottom chord, d = joist depth. Substituting Equation 3.3 into Equation 3.4 gives

$$P = (NF)\ L^2 / 8\ d\ s' \tag{3.5}$$

thus,

$$NF = 8\ P\ d\ s' / L^2 \tag{3.6}$$

Assuming that stress in the top chord is uniform over the chord,

$$f_a = P/A = (NF)\ L^2 / 8\ s'\ A\ d \tag{3.7}$$

where $f_a$ = top chord axial stress, A = top chord cross-sectional area. Finally, using Equations 3.1 and 3.5, the joist normal uniform load is found to be a function of chord axial load

$$w = 8\ P\ d / L^2 \tag{3.8}$$

The lateral restraining force per clip spacing is obtained by substituting (NF) from Equation 3.6 into the experimentally determined friction force equations (Equations 2.3, 2.4 and 2.5). For instance, for 3 in. clips without insulation

$$FF = 38.91 + 0.2454\ (8Pds'/L^2) - 4.396 \times 10^{-6}(8Pds'/L^2)^2 \tag{3.9}$$

Assuming that the buckled shape of the top chord is a sinusoidal curve, the deflected shape between bridging lines is given by

$$y = B \sin (\pi x/S) \tag{3.10}$$

where y = lateral deflection of the top chord due to buckling for a point located a distance x from the left hand side support (see Figure 3.4), B = deflection at mid-distance between bridging points. The lateral deflected shape of the top chord due to a series of concentrated forces can also be calculated. Setting the midspan deflection from this loading equal to B in Equation 3.10 results in the maximum deflection that the frictional forces can resist. The deflection due to a series of concentrated forces could be approximated by a sinusoidal curve as the one given in Equation 3.10. The value of B is determined using the energy method as explained herein. The potential energy of the chord with a series of concentrated forces (FF) is given by

$$W + U = EI_y \int_0^S (y'')^2 \, dx - \sum_{i=1}^{n} B\,(FF)\,\sin(\pi x_i / S) \qquad (3.11)$$

where W = external work done by frictional forces (FF), U = internal bending strain energy, n = number of clips between bridging lines, $I_y$ = moment of inertia of top chord about its vertical centroidal axis, $x_i$ = distance between left support and load number i, see Figure 3.4, y" = 2nd derivative of displacement y, with respect to x, $y'' = -B\,\pi^2/S^2 \sin(\pi x/S)$. Taking first derivative of (W+U) with respect to B in Equation 3.11 and setting it equal to zero gives

$$\partial(W+U)/\partial B = \pi^4 EI_y / 2S^3 \; B - (FF) \sum_{i=1}^{n} \sin(\pi x_i/S) = 0 \qquad (3.12)$$

solving for B gives

$$B = 2(FF)S^3/\pi^4 EI_y \sum_{i=1}^{n} \sin(\pi x_i/S) \qquad (3.13)$$

It is worth mentioning that the deflections due to the concentrated forces could have been "exactly" calculated using statics. However, it was desired that the deflection be represented by a sine curve in order to equate

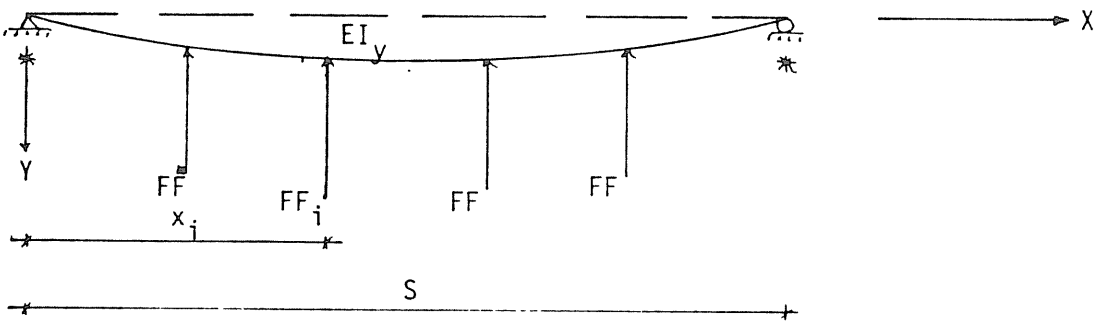


Figure 3.4 Top Chord With Clip Forces Acting on It

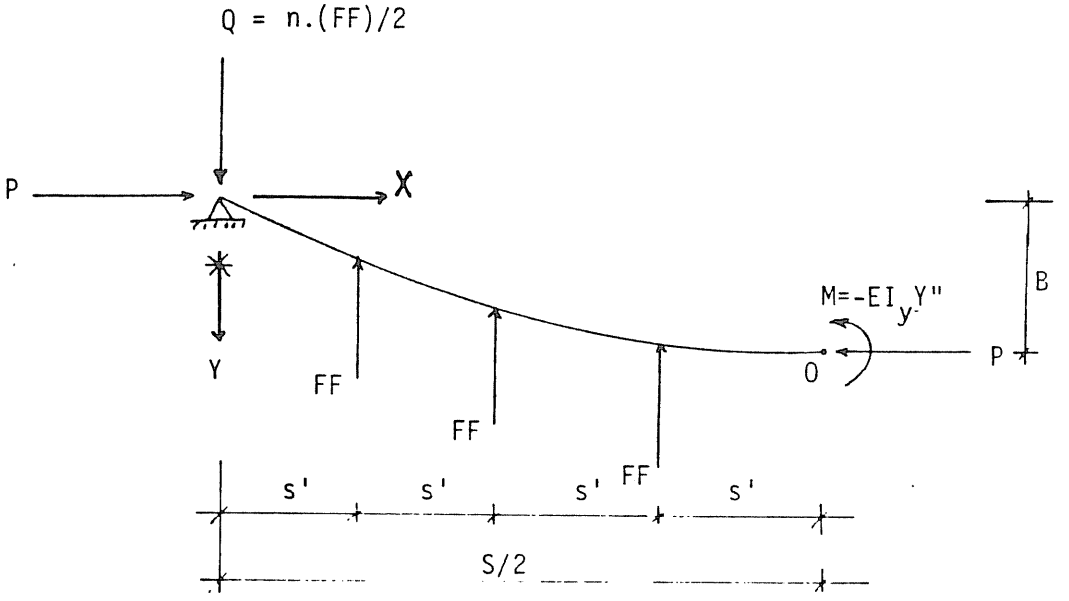


Figure 3.5 Free Body Diagram For Top Chord After Buckling

it to the deflected shape due to buckling.

The free body diagram of the deflected chord can now be studied and equilibrium conditions formulated, see Figure 3.5. Summing moments about point 0 gives

$$M = PB + \{\Sigma\ (FF)\ x_i\ \} - S/2\ n/2\ (FF) \qquad (3.14)$$

where B is defined by Equation 3.13, $x_i$ = distance from point 0 to point of clip force i application (see Figures 3.4 and 3.5),

$$x_i = s'\ \{0.5 + (i-1)\} \qquad \text{for n=even} \qquad (3.15a)$$

$$x_i = s'(i) \qquad \text{for n=odd} \qquad (3.15b)$$

assuming elastic conditions at mid-distance between bridging lines

$$M = -\ EI_y\ y'' \qquad (3.16)$$

Substituting Equation 3.10 into Equation 3.16 gives

$$M = EI_y B\ \pi^2/S^2\ \sin(\pi x/S) \qquad (3.17a)$$

and at x = S/2

$$M = EI_y\ B\pi^2/S^2 \qquad (3.17b)$$

Substituting Equations 3.17 and 3.15 into Equation 3.14 results in equilibrium equation at mid-distance between bridging lines

$$EI_y B\ \pi^2/S^2 - \sum_{i=1}^{n/2}(FF)s'\{0.5+(i-1)\} = PB - nS(FF)/4 \quad \text{for n=even} \qquad (3.18a)$$

$$EI_y B\ \pi^2/S^2 - \sum_{i=1}^{n-1/2}(FF)s'i = PB - nS(FF)/4 \qquad \text{for n=odd} \qquad (3.18b)$$

From Equations 3.18, the elastic buckling laod $P_E$ can be calculated

$$P_E = \pi^2\ EI_y/S^2 - (FF)/B\ \sum_{}^{n/2} s'\{0.5+(i-1)\}+nS(FF)/4B \quad \text{for n=even} \qquad (3.19a)$$

$$P_E = \pi^2\ EI_y/S^2 - (FF)/B \sum_{i=1}^{n-1/2} s'i + nS(FF)/4B \qquad \text{for n=odd} \qquad (3.19b)$$

The elastic buckling load calculated above is equal to the actual buckling load $P_{cr}$ for slender chords (i.e., large bridging spacing and small radius of gyration). However, for short stocky columns inelastic buckling is the governing mode. To incorporate the inelastic effects, the Column Research Council (CRC) recommendations are used[8]:

$$P_{cr} = P_E \qquad \text{for } P_E < P_p \qquad (3.20a)$$

$$P_{cr} = P_I \qquad \text{for } P_E > P_p \qquad (3.20b)$$

where $P_{cr}$= chord critical load, $P_I$= inelastic buckling load = $P_y - P_y^2/4P_E$, $P_y$= chord yield load, $P_p$= proportional limit load. The CRC suggests that $P_p$ be taken as

$$P_p = 0.5\ P_y \qquad (3.21)$$

With the critical load, $P_{cr}$, the associated uniform load can be calculated using Equation 3.8. Example calculations are given in the next section and predicted failure loads for the forty-six tests reported in Reference 2 are given in Chapter IV.

3.2.3 Example Calculations

The configuration for Test 40/3/20-14W of Reference 2 is used to demonstrate the required calculations. The required data is as follows:

Material Data: E=29000 ksi, $F_y$=57.9 ksi

Joist Data: $I_x$=118.05 $in.^4$, d=18.9 in.

Top Chord Data: $I_y$=0.551 $in.^4$, A=0.68 $in.^2$

Clip Data: 3 in. clip without insulation, s'=24 in.

Bridging Data: S=10 ft.

From the bridging and clip spacing, the restraining forces are located as shown in Figure 3.6 and n = 4. Using Equation 3.19a for the critical

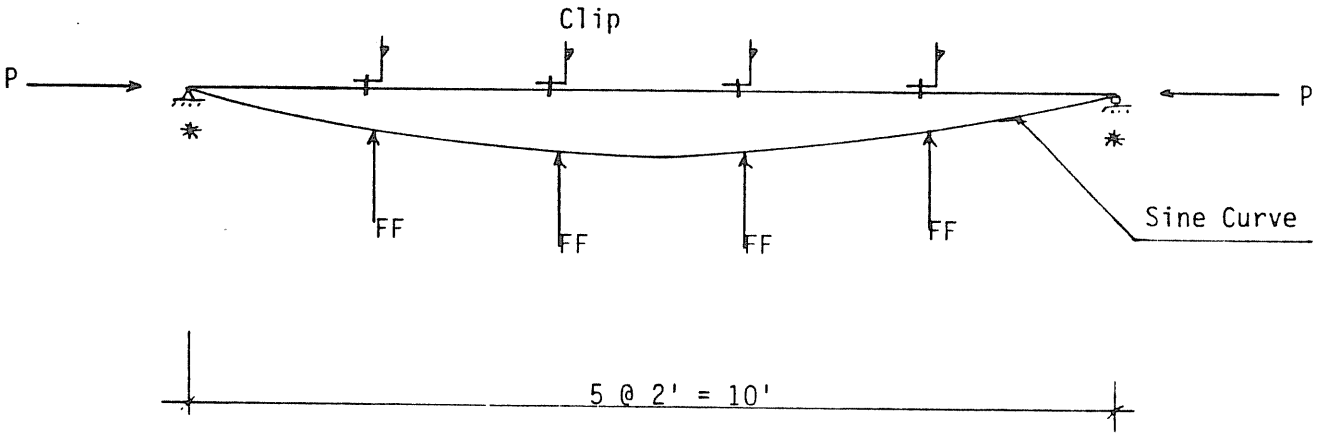


* Bridging Lines Locations

Figure 3.6 Restraining Forces, Example Configuration

elastic load determination gives

$$P_E = \pi^2 \frac{29000 \times 0.551}{(10 \times 12)^2} - \frac{(FF)}{B} \sum_{i=1}^{2} 24\{0.5+(i-1)\}+4 \frac{120(FF)}{4B} \quad (3.22a)$$

or

$$P_E = 10.95 + 72.0 \frac{(FF)}{B} \quad (3.22b)$$

B is determined from Equation 3.13, which gives

$$B = \frac{2(FF)(120)^3}{\pi^4 x 29000 x 0.551} \sum_{i=1}^{4} \sin(\pi x_i/120) \quad (3.23a)$$

where $x_1$= 24 in., $x_2$= 48 in., $x_3$= 72 in., $x_4$= 96 in., thus

$$B = 6.83\ (FF) \quad (3.23b)$$

Substituting Equation 3.23b into Equation 3.22b gives (note that the frictional force (FF) cancels in the resulting equation):

$$P_E = 21.50 \text{ kips} \quad (3.24a)$$

but

$$P_p = 0.5 \times 57.9 \times 0.68 = 19.69 \text{ kips} \quad (3.24b)$$

since $P_E > P_p$ then

$$P_{cr} = P_I = (57.9x0.68) - \frac{(57.9x0.68)^2}{4x21.50} = 21.35 \text{ kips} \quad (3.24c)$$

Finally, the associated uniform load on the joist is calculated using equation 3.8

$$w = \frac{8x21.35x18.90}{(40x12)^2} = 0.014 \text{ k/in.} = 168.1 \text{ lb/ft} \quad (3.24d)$$

## 3.3 Modified Newmark's Iterative Method

### 3.3.1 Discussion

A second analysis procedure is developed using the top chord

model shown in Figure 3.7. In this figure, p is the distance between two adjacent panel points and the loads bP, cP, ..., $\alpha$P are the horizontal components of the web forces. It is noted that the sum a+b+...+$\alpha$ must equal unity. Springs 1 through 4 are added to simulate the web restraining effect acting at each panel point. The stiffness K is the web lateral stiffness at each panel point. The numerical iterative procedure developed by Newmark and suggested by Godden[9] is used to determine the top chord buckling load. This procedure can be used to determine the buckling load for a column with any axial load variation and any number of springs acting on the column. The development and application of this procedure to open web steel joists is explained in the next section.

3.3.2 Method Development

It is possible to determine the deflections in a beam, or a column, at discrete points due to a given loading using a procedure called "Forward Integration"[9]. This procedure is a numerical one; however, it possesses a theoretical basis. It is also possible to apply this procedure to critical load determination for open web steel joists with few modifications. The procedure applies to beams with transverse loading, columns with constant axial compressive load, columns with several axial loads and columns with several axial loads and several elastic springs.

For a beam with transverse loads acting as shown in Figure 3.8, the shear in regions 1, 2, 3 and 4 is given by

$$\text{Shear}_i = V_a + \sum_{i=1}^{i} V_i \qquad (3.25)$$

where $V_a$ is the value of shear at A. The change of moment in each region is equal to the magnitude of the shear in that region times the length of

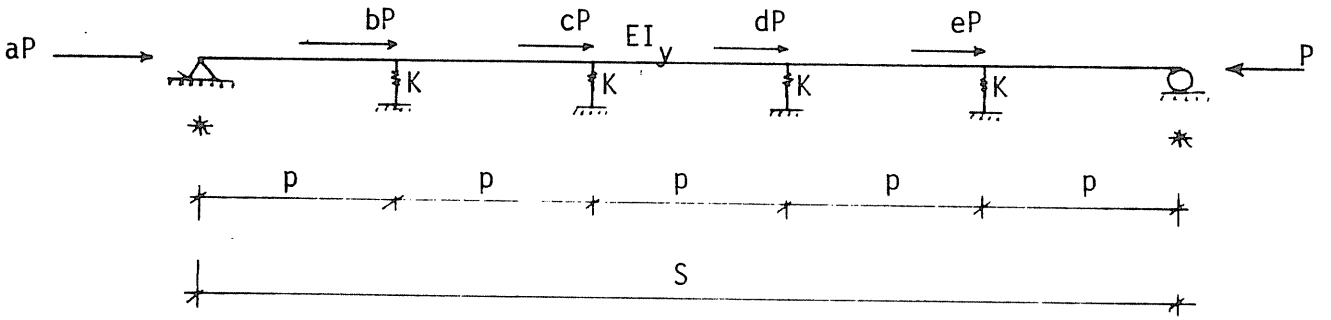


Figure 3.7 Top Chord Configuration Including Web and Axial Load Variation Effects

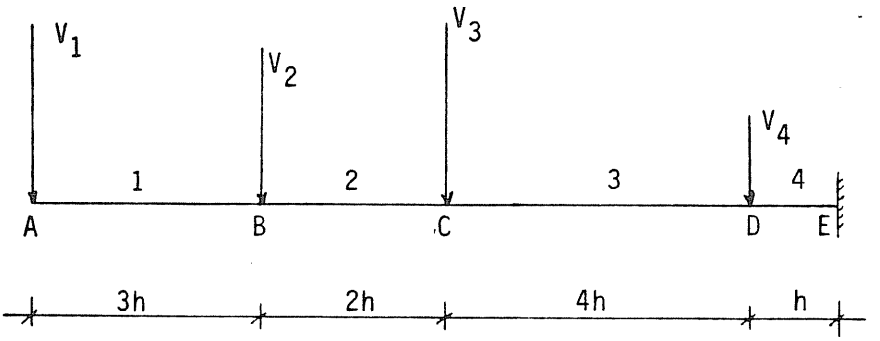


Figure 3.8 Cantilever Beam With Concentrated Loads

(a) Linear Loading, Equal Chords

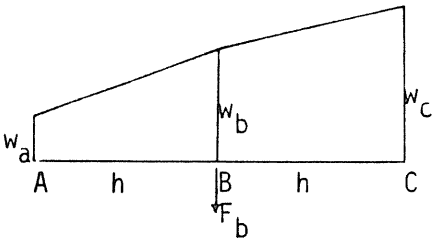


$$F_b = \frac{h}{6}(w_a + 4w_b + w_c)$$

(b) Parabolic Loading, Equal Chords

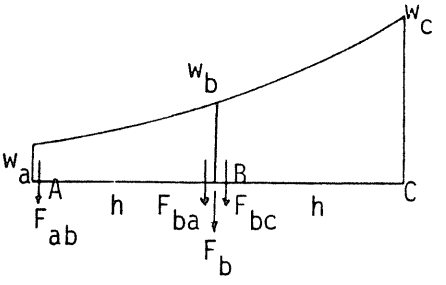


$$F_{ab} = \frac{h}{24}(7w_a + 6w_b - w_c)$$

$$F_{ba} = \frac{h}{24}(3w_a + 10w_b - w_c)$$

$$F_b = \frac{h}{12}(w_a + 10w_b + w_c)$$

Figure 3.9 Nodal Concentration Functions Due to Linear and Parabolic Force Variations

the region. For example, the moment increment to the left of point C is equal to

$$\Delta M_c = (V_1+V_2)(2h) \tag{3.26}$$

where 2h = width of region 2. After the change in moment in each region is calculated, the moments at points A, B, C, D and E are calculated by simply adding the moment at each point to all moments prior to it, or

$$M_i = \sum_{j=1}^{i} \Delta M_j \tag{3.27}$$

The values of curvature, y", are then calculated by dividing the moment at each point by the associated flexural stiffness, EI. The "nodal concentration", "Y", is then calculated using one of the equations shown in Figure 3.9. The nodal concentration of a function is the concentrated force that would produce the same shear and moment as a distributed force having the same distribution as that function[10]. Values of nodal concentration for linear and parabolic functions acting on equally divided members are given in Figure 3.9. Nodal concentration of more complicated functions are reported in References 9 and 10. These formulas are based on Simpson's rule. The slope, y', can be found from Y" values using the equation

y'(in a region) = Y"(in that region) x length of that region (3.28)

Deflection increments can be calculated from y' in a similar manner (e.g., deflection increment(region 2) = y'(region 2) x length(region 2)). The deflection at a node then calculated using the deflection increments, for example,

$$y_c = \{ \sum_{i=1}^{4} (\Delta y_i) \} - (\Delta y_a + \Delta y_b) \qquad (3.29)$$

The calculated deflections are then adjusted to satisfy the boundary conditions (e.g., deflection=0 at supports) by adding or subtracting corrections to all nodes if necessary.

This method can be applied to columns in a similar manner but with slight modification. The column is first divided into regions, preferably of equal length, then a buckled mode is assumed and deflections at points between regions are estimated according to the assumed buckled mode. The second order moments are then calculated at all points due to the axial loads acting on the column. Once the moments are calculated, the analysis becomes identical to the one described above. A numerical example of this type of problem is given in Figure 3.10. In that figure, the assumed deflection, $y_a$, at midspan is "e", whereas the calculated deflection, $y_c$, is equal to "$5ePh^2/12EI$". By equating $y_a$ to $y_c$, the critical load is calculated as follows:

$$1.0\ e = 5.0\ e\ Ph^2/12EI \qquad (3.30a)$$

but, since the column is divided into two regions,

$$h = L/2 \qquad (3.30b)$$

thus

$$P_{cr} = 9.60\ EI/L^2 \qquad (3.30c)$$

The exact solution for this problem is $P_{cr} = \pi^2 EI/L^2 = 9.87\ EI/L^2$. The value obtained from this method using only two regions is equivalent to a 2.8% error. If higher level of accuracy is desired, the number of regions is increased. It can be shown that when four regions are used,

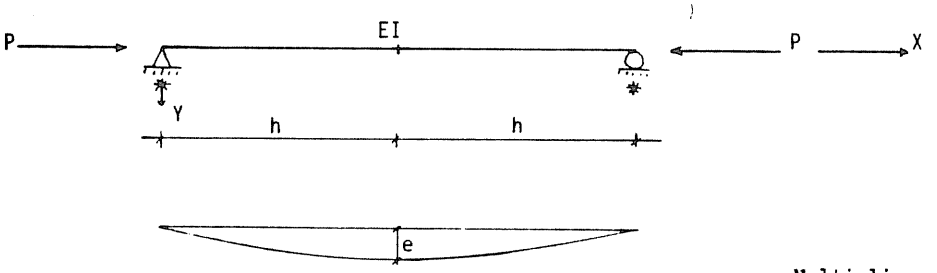


| | | | | |
|---|---|---|---|---|
| | | | | Multiplier |
| Assumed Buckling Shape | 0.0 | 1.0 | 0.0 | e |
| M | 0.0 | 1.0 | 0.0 | eP |
| y"=M/EI | 0.0 | 1.0 | 0.0 | eP/EI |
| Nodal Concentration Y" | 0.0 | 10.0 | 0.0 | ePh/12EI |
| y' | 5.0 | | -5.0 | ePh/12EI |
| Calculated Deflection | 0.0 | 5.0 | 0.0 | $ePh^2/12EI$ |

Figure 3.10 Buckling Load Determination for an Axially Loaded Column Using Newmark's Method

$P_{cr} = 9.85\ EI/L^2$ which is equivalent to only 0.16% error.

This method can be generalized for use with any type of column and any axial force distribution. In the previous example, the exact buckling mode was assumed initially, however, for more complicated problems that mode is usually unknown. In these instances, an iterative procedure is required with an assumed buckling mode for the first cycle. If the calculated deflected shape does not coincide with the assumed one, the calculated shape is taken as the new shape, and the analysis is repeated. The process is repeated until the calculated buckled shape is equal to the assumed buckled shape with an acceptable degree of tolerance. The critical load can then be calculated in the manner described previously.

The method can also be generalized to determine the critical load for a column with axial loads and elastic springs. In such cases, the analysis is divided into two steps: (1) axial load effect (as explained previously), (2) spring forces effect. The spring force analysis is identical to the axial force analysis with the exception of the way moments are calculated. In the former, the forces in the springs due to the assumed deflection are determined, and then moments due to these forces are calculated, see Figure 3.11. Finally, by setting the assumed deflection equal to the summation of the calculated deflections due to axial and spring forces, the critical load is calculated as follows:

$$1.0\ e = 5.0\ ePh^2/12EI - 1.0\ ekh^3/6EI \qquad (3.31a)$$

but

$$h = L/2 \qquad (3.31b)$$

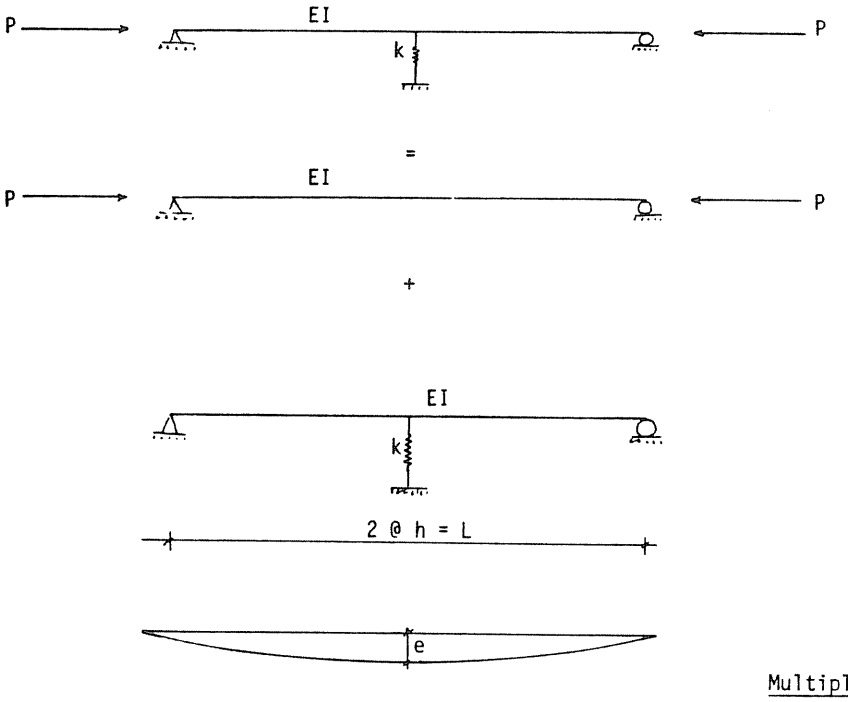


| | | | | Multiplier |
|---|---|---|---|---|
| Assumed Buckling Shape | 0.0 | 1.0 | 0.0 | e |
| Spring Force | 0.0 | 1.0 | 0.0 | ek |
| M | 0.0 | -0.5 | 0.0 | ekh |
| y"=M/EI | 0.0 | -0.5 | 0.0 | ekh/EI |
| Nodal Concentration Y" | 0.0 | -2.0 | 0.0 | $ekh^2/6EI$ |
| y' | -1.0 | | +1.0 | $ekh^2/6EI$ |
| Calculated Deflection | 0.0 | -1.0 | 0.0 | $ekh^3/6EI$ |

Figure 3.11 Buckling Load Determination for a Column With Elastic Spring Effect Included

thus

$$P_{cr} = 9.60\ EI/L^2 + 0.20\ KL \qquad (3.31c)$$

To apply this method to open web joists and light trusses, the lateral stiffness of the web members at panel points, K, must be determined. The stiffness of a web member is assumed to be equivalent to the stiffness of a fixed-fixed column having the same moment of inertia, length and modulus of elasticity as the web member, that is

$$k_w = 12\ EI_w/L_w^3 \qquad (3.32)$$

where $k_w$= lateral stiffness of one web member, $I_w$= moment of inertia of the web member about an axis in the plane of the joist and perpendicular to the web member, and $L_w$= length of the web member. Since two web members meet at each panel point, the spring stiffness acting on the top chord is equal to the summation of the stiffnesses of both web members, or

$$K = k_{w1} + k_{w2} = 12E(I_{w1}/L_{w1}^3 + I_{w2}/L_{w2}^3) \qquad (3.33)$$

An example of application of this method to open web steel joists is given in Appendix A.

## 3.4 Conclusion From Theoretical Study

Two analytical methods were developed to study light trusses and open web steel joists behavior. The first method is "approximate" and it considers the standing seam roof panels and clips effect on the joists; whereas the second method is "exact", but it only considers the web restraining effect and the top chord force variation. The latter method does not consider the standing seam roof components (e.g., clip

and panel) because the restraining force provided by that roof system is frictional in nature and is independent of the top chord displacement. The predicted failure loads for all forty-six experimental tests reported in Reference 2 using both methods are given and compared to the actual failure loads in Chapter IV. In addition, a design equation is developed based on the method that is believed to be more accurate, and the results from this equation are compared to the experimental failure loads.

# CHAPTER IV

## COMPARISON OF EXPERIMENTAL TO NEW DESIGN PROCEDURE RESULTS

### 4.1 General

Simulated gravity loading tests conducted at the Fears Structural Engineering Laboratory[2] serve as the basis of comparison for the results obtained using the two analysis procedures developed in Chapter III. All comparisons are made without including a factor of safety, therefore, an ideal case is one in which the ratio of experimental to predicted failure load is equal to unity. A ratio greater than one indicates a conservative case and a ratio less than one indicates an unconservative case.

### 4.2 Clip-Frictional Force Method Results

A computer program was developed based on the method described in Section 3.2. A listing of this program is given in Appendix B. Predicted failure loads for joists tested are compared with the experimental failure loads. The results are given in Tables 4.1, 4.2 and 4.3 for 40 ft., 50 ft. and 60 ft. span joists, respectively. The results are summarized below.

40 ft. Span Tests. As mentioned previously, rod and angle web joists designed for nominal 20 and 40 psf live loads at 5 ft. joist spac-

Table 4.1
Clip-Frictional Force Method Results for 40 ft. Span Joists

| | | Test No. | Bridging Spacing (ft.) | $(kS/r)_y$ | Insulation | Exp. $w_E$ (plf) | Theoretical $w_T$ (plf) | Theoretical $w_E/w_T$ |
|---|---|---|---|---|---|---|---|---|
| 20 psf | Rod web | 40/3/20-12 | 20.0 | 270.2 | N | 208.7 | 35.8 | 5.83 |
| | | 40/3/20-13 | 10.0 | 137.5 | N | 278.1 | 159.3 | 1.75 |
| | | 40/3/20-14 | 10.0 | 131.7 | N | 238.2 | 166.2 | 1.43 |
| | | 40/3/20-15 | 10.0 | 138.5 | N | 268.0 | 147.3 | 1.82 |
| | Angle web | 40/3/20-34[1] | 10.0 | 114.7 | N | 284.9 | | |
| | | 40/3/20-35 | 10.0 | 119.6 | N | 235.9 | 193.2 | 1.22 |
| | | 40/3/20-36 | 10.0 | 115.8 | I | 254.5 | 204.1 | 1.25 |
| 40 psf | Rod Web | 40/3/40-40 | 10.0 | 125.6 | N | 421.2 | 298.4 | 1.41 |
| | | 40/3/40-41 | 10.0 | 123.2 | N | 418.1 | 287.6 | 1.45 |
| | | 40/3/40-42 | 10.0 | 123.4 | I | 433.5 | 294.3 | 1.47 |
| | | 40/3/40-45 | 10.0 | 120.7 | R | 340.9 | 294.1 | 1.16 |
| | Angle web | 40/3/40-37[1] | 10.0 | 100.7 | N | 302.2 | | |
| | | 40/3/40-38[1] | 10.0 | 101.4 | N | 417.2 | | |
| | | 40/3/40-39 | 10.0 | 102.2 | N | 385.9 | 340.1 | 1.13 |
| | | 40/3/40-43 | 10.0 | 105.8 | N | 382.4 | 335.2 | 1.14 |
| | | 40/3/40-44 | 10.0 | 102.0 | I | 376.3 | 352.5 | 1.07 |
| | | 40/3/40-46 | 10.0 | 106.9 | R | 347.3 | 338.4 | 1.03 |
| * | | 40/3/20-11 | 20.0 | 265.3 | N | 314.2 | 43.9 | 7.15 |

*Retest of Test 40/3/20-11

[1]Test not considered to be valid

N = w/o insulation

I = w/ insulation

R = RIS Beams

Table 4.2
Clip-Frictional Force Method Results for 50 ft. Span Joists

| | | Test No. | Bridging Spacing (ft.) | $(kS/r)_y$ | Insulation | Exp. $w_E$ (plf) | Theoretical | |
|---|---|---|---|---|---|---|---|---|
| | | | | | | | $w_T$ (plf) | $w_E/w_T$ |
| Angle web | 40 psf | 50/3/40-31 | 9.90 | 100.7 | N | 264.1 | 341.6 | 0.77 |
| | | 50/3/40-33 | 9.90 | 101.1 | N | 367.7 | 335.8 | 1.09 |
| | | 50/3/40-29 | 6.30 | 62.2 | N | 422.2 | 417.9 | 1.01 |
| | | 50/3/40-30 | 6.30 | | | 347.6* | | |
| | | 50/3/40-32 | 6.30 | 64.3 | N | 349.3 | 404.7 | 0.86 |
| | | 50/3/40-28 | 5.20 | | | 334.8* | | |
| | | 50/3/40-27 | 4.60 | | | 334.2* | | |

* Not conducted to failure

Table 4.3
Clip-Frictional Force Method Results for 60 ft. Span Joists

| | | Test No. | Bridging Spacing (ft.) | $(kS/r)_y$ | Insulation | Exp. $w_E$ (plf) | Theoretical | |
|---|---|---|---|---|---|---|---|---|
| | | | | | | | $w_T$ (plf) | $w_E/w_T$ |
| Angle web | 20 psf | 60/3/20-4 | 30.0 | 373.8 | N | 110.0 | 18.9 | 5.81 |
| | | 60/4/20-1 | 20.0 | 243.1 | I | 111.7 | 42.1 | 2.65 |
| | | 60/4/20-2 | 20.0 | 242.0 | I | 111.7 | 39.1 | 2.86 |
| | | 60/3/20-5 | 15.0 | 179.0 | N | 162.9 | 84.0 | 1.94 |
| | | 60/3/20-6 | 13.2 | 155.1 | N | 170.5 | 103.2 | 1.65 |
| | | 60/3/20-3 | 13.2 | 169.6 | N | 123.0 | 86.9 | 1.42 |
| | | 60/3/20-7 | 10.0 | 115.0 | N | 197.8 | 175.9 | 1.12 |
| | | 60/3/20-8 | 10.0 | 117.6 | N | 138.4 | 174.3 | 0.79 |
| | | 60/3/20-9 | 9.3 | 114.9 | N | 128.9 | 174.6 | 0.74 |
| | | 60/3/20-16 | 9.3 | 113.7 | N | 133.5 | 167.6 | 0.80 |
| | | 60/3/20-17 | 7.6 | 90.1 | N | 210.4 | 206.4 | 1.02 |
| | | 60/3/20-18 | 7.6 | 94.3 | N | 148.3 | 208.6 | 0.71 |
| | | 60/3/20-26 | 7.7 | 90.9 | N | 153.2 | 206.9 | 0.74 |
| | | 60/3/20-19 | 6.0 | 74.8 | N | 163.1 | 224.6 | 0.73 |
| | | 60/3/20-20 | 4.0 | 48.3 | N | 180.4 | 238.4 | 0.76 |
| | | 60/3/20-21 | 4.0 | 48.3 | N | 187.8 | 237.5 | 0.79 |
| | 40 psf | 60/3/40-10 | 10.4 | 102.4 | N | 316.5 | 312.3 | 1.01 |
| | | 60/3/40-24 | 7.7 | 75.0 | R | 306.6 | 350.9 | 0.87 |
| | | 60/3/40-25 | 7.7 | 74.4 | R | 309.1 | 355.2 | 0.87 |
| | | 60/3/40-23 | 4.0 | 39.4 | N | 399.3 | 387.6 | 1.03 |
| | | 60/3/40-22 | 4.0 | 39.4 | N | 411.8 | 387.6 | 1.06 |

ing were tested. From Table 4.1, the ratio of $w_E/w_T$ ranged from 1.41 to 1.82 for rod web joist tests with 10 ft. bridging spacing and without insulation. The corresponding top chord slenderness ratios ranged from 120.7 to 138.5. The ratio of $w_E/w_T$ ranged from 1.13 to 1.26 for angle web joists with 10 ft. bridging spacing and without insulation. The corresponding top chord slenderness ratios ranged from 100.7 to 119.6. The ratio of $w_E/w_T$ was 5.83 for Test 12 where bridging spacing was 20 ft. and the top chord slenderness ratio was 270.2. It is noted, however, that the AISC and the SJI specifications do not permit slenderness ratios above 200 for compression members[1,3].

It was reported in Reference 2 that the failure mode for all 40 ft. span joists, except for Tests 34, 37 and 38, was out-of-plane lateral buckling of the top chord. However, the buckled shape for rod web joists was always a smooth curve between bridging lines, whereas for angle web joists buckling occurred at the first panel point next to midspan bridging lines, see Figure 4.1.

50 ft. Span Tests. Four 40 psf angle web joists were tested. From Table 4.2, the ratio of $w_E/w_T$ ranged from 0.77 to 1.09 with bridging spacing between 4.6 and 9.9 ft. The corresponding top chord slenderness ratios ranged from 62.2 to 100.7. The failure mode for all tests was reported to be as shown in Figure 4.1b.

60 ft. Span Tests. Sixteen 20 psf and five 40 psf angle web joists were tested. From Table 4.3, the ratio of $w_E/w_T$ ranged from 0.71 to 5.81 with bridging spacing varying between 4 ft. and 30 ft. for the nominal 20 psf tests. The corresponding top chord slenderness ratios ranged from 48.3 to 373.8. The ratio of $w_E/w_T$ ranged from 0.87 to

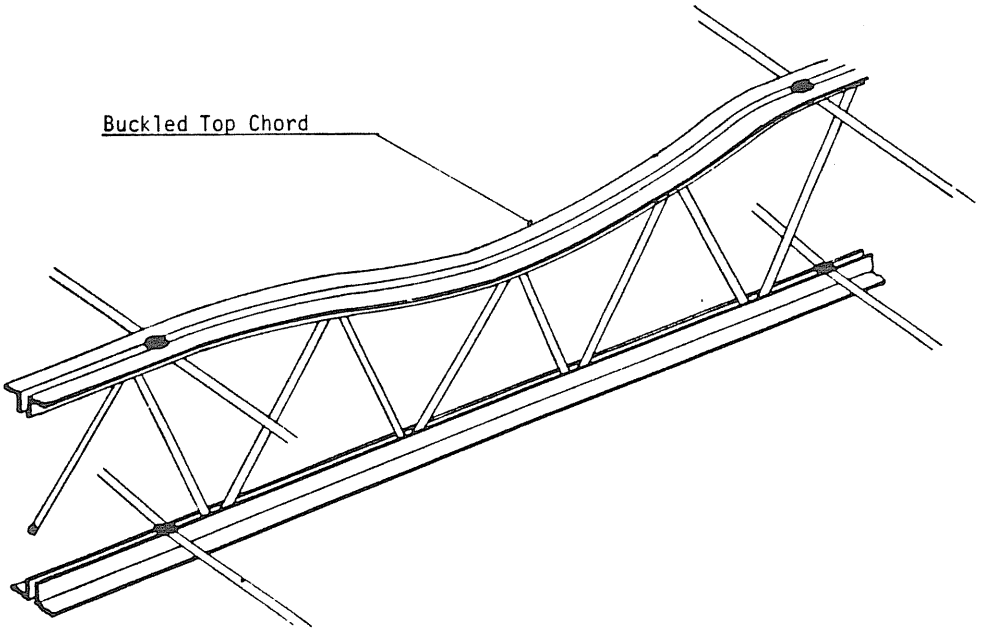


(a) Typical Rod Web Joist Failure Mode

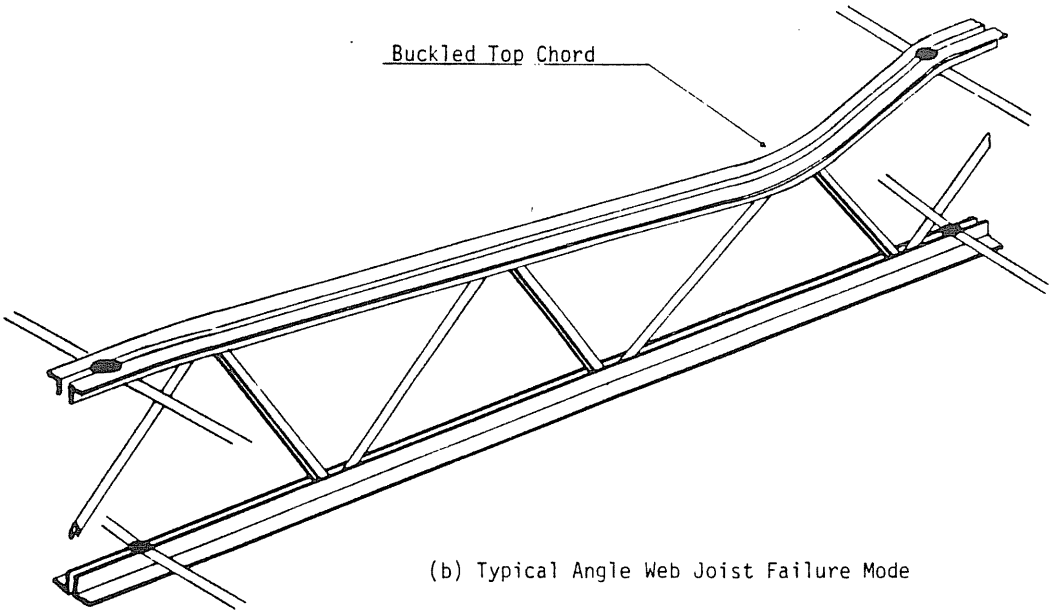


(b) Typical Angle Web Joist Failure Mode

Figure 4.1 Rod and Angle Web Joists Typical Failure Modes

1.06 with bridging spacing between 4 ft. and 10.4 ft. for the nominal 40 psf tests. The corresponding top chord slenderness ratios ranged from 39.4 to 102.4. The failure mode for all valid tests was reported to be as shown in Figure 4.1b.

## 4.3 Modified Newmark's Iterative Method Results

A computer program was developed based on the method described in Section 3.3. A listing of this program is given in Appendix C. Analytical results are compared to experimental results found in Reference 2. The top chord axial force variation between bridging lines was determined from the results shown in Figure 3.2. The lateral web stiffness at panel points was determined using the web configurations shown in Figure 4.2 and data given in Reference 2. Calculated web stiffnesses for the 40 ft. span rod and angle web, 50 ft. span angle web and 60 ft. span angle web joists are given in Tables 4.4, 4.5 and 4.6, respectively. Predicted failure loads are compared with experimental failure loads reported in Reference 2 and the results are given in Tables 4.7, 4.8 and 4.9 for 40 ft., 50 ft. and 60 ft. span joists, respectively. The results are summarized below.

40 ft. Span Tests. From Table 4.7, the ratio of $w_E/w_T$ ranged from 1.18 to 1.41 for rod web joist tests with 10 ft. bridging spacing and without insulation. The corresponding top chord slenderness ratios ranged from 120.7 to 138.5. The ratio of $w_E/w_T$ ranged from 1.05 to 1.13 for angle web joist tests with 10 ft. bridging spacing and without insulation. The corresponding top chord slenderness ratios ranged from 100.7 to 119.6. The ratio of $w_E/w_T$ was 0.77 for Test 12 where the bridging spacing was 20 ft. and the corresponding top chord

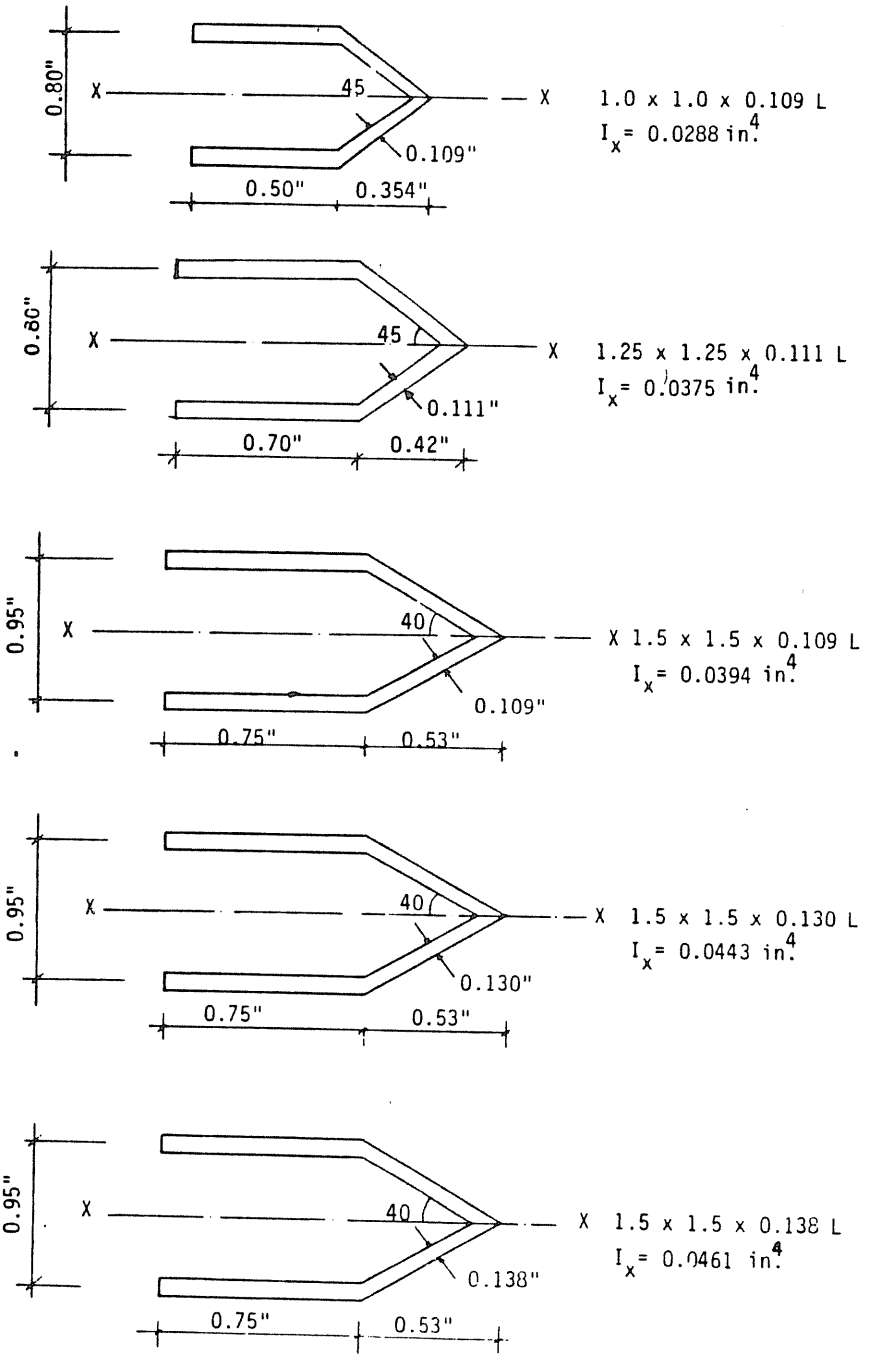


Figure 4.2 Crimped Angle Web Members Lateral Stiffnesses

Table 4.4

40 ft. Span Joists Web Stiffness

| | | Member | $I_w$ ($in.^4$) | $L_w$ (in.) | K (k/in) |
|---|---|---|---|---|---|
| 20 psf | Rod | 9/16 $\phi$ in. | 0.00491 | 23.32 | 0.2695 |
| | Angle* | L 1x1x.109 (T) | 0.0288 | 31.24 | 0.757 |
| | | L 1¼x1¼x.111 (C) | 0.0375 | | |
| 40 psf | Rod | 5/8 $\phi$ in. | 0.00749 | 23.32 | 0.4111 |
| | Angle* | L 1x1x.109 (T) | 0.0288 | 31.24 | 0.778 |
| | | L 1½x1½x.109 (C) | 0.0394 | | |

Table 4.5

50 ft. Span Joists Web Stiffness

| | | Member | $I_w$ ($in.^4$) | $L_w$ (in.) | K (k/in) |
|---|---|---|---|---|---|
| 40 psf | Angle* | L 1x1x.109 (T) | 0.0288 | 35.38 | 0.574 |
| | | L 1½x1½x.130 (C) | 0.0443 | | |

Table 4.6

60 ft. Span Joists Web Stiffness

| | | Member | $I_w$ ($in.^4$) | $L_w$ (in.) | K (k/in) |
|---|---|---|---|---|---|
| 20 psf | Angle* | L 1x1x.109 (T) | 0.0288 | 38.42 | 0.419 |
| | | L 1½x1½x.109 (C) | 0.0394 | | |
| 40 psf | Angle* | L 1x1x.109 (T) | 0.0288 | 38.42 | 0.460 |
| | | L 1½x1½x.138 (C) | 0.0461 | | |

* See Figure 4.1 for $I_w$ calculations
(T) indicates a tension web member
(C) indicates a compression web member

Table 4.7
Modified Newmark's Method Results for 40 ft. Span Joists

| | | Test No. | Bridging Spacing (ft.) | $(kS/r)_y$ | Insulation | Exp. $w_E$ (plf) | Theoretical | | Approximate | | |
|---|---|---|---|---|---|---|---|---|---|---|---|
| | | | | | | | $w_T$ (plf) | $w_E/w_T$ | $w_A$ (plf) | $w_E/w_A$ | $w_T/w_A$ |
| 20 psf | Rod web | 40/3/20-12 | 20.0 | 270.2 | N | 208.7 | 271.8 | 0.77 | 271.7 | 0.77 | 1.00 |
| | | 40/3/20-13 | 10.0 | 137.5 | N | 278.1 | 205.4 | 1.35 | 197.9 | 1.41 | 1.04 |
| | | 40/3/20-14 | 10.0 | 131.7 | N | 238.2 | 201.8 | 1.18 | 195.5 | 1.22 | 1.03 |
| | | 40/3/20-15 | 10.0 | 138.5 | N | 208.0 | 190.7 | 1.41 | 184.8 | 1.45 | 1.03 |
| | Angle web | 40/3/20-34[1] | 10.0 | 114.7 | N | 284.9 | | | | | |
| | | 40/3/20-35 | 10.0 | 119.6 | N | 235.9 | 225.5 | 1.05 | 227.0 | 1.04 | 0.99 |
| | | 40/3/20-36 | 10.0 | 115.8 | I | 254.5 | 236.4 | 1.08 | 237.9 | 1.07 | 0.99 |
| 40 psf | Rod Web | 40/3/40-40 | 10.0 | 125.6 | N | 421.2 | 332.0 | 1.27 | 323.9 | 1.30 | 1.03 |
| | | 40/3/40-41 | 10.0 | 123.2 | N | 418.1 | 326.0 | 1.28 | 309.4 | 1.35 | 1.05 |
| | | 40/3/40-42 | 10.0 | 123.4 | I | 433.5 | 325.8 | 1.33 | 316.9 | 1.37 | 1.03 |
| | | 40/3/40-45 | 10.0 | 120.7 | R | 340.9 | 327.0 | 1.04 | 318.9 | 1.07 | 1.03 |
| | Angle web | 40/3/40-37[1] | 10.0 | 100.7 | N | 302.2 | | | | | |
| | | 40/3/40-38[1] | 10.0 | 101.4 | N | 417.2 | | | | | |
| | | 40/3/40-39 | 10.0 | 102.2 | N | 385.9 | 341.6 | 1.13 | 343.3 | 1.12 | 0.99 |
| | | 40/3/40-43 | 10.0 | 105.8 | N | 382.4 | 338.1 | 1.13 | 340.0 | 1.12 | 0.99 |
| | | 40/3/40-44 | 10.0 | 102.0 | I | 376.3 | 342.6 | 1.10 | 344.2 | 1.09 | 1.00 |
| | | 40/3/40-46 | 10.0 | 106.9 | R | 347.3 | 342.6 | 1.01 | 344.6 | 1.01 | 1.00 |
| * | | 40/3/20-11 | 20.0 | 265.3 | N | 314.2 | 320.4 | 0.98 | 320.4 | 0.98 | 1.00 |

*Retest of Test 40/3/20-11

[1]Test not considered to be valid

N = w/o insulation

I = w/ insulation

R = RIS Beams

$w_E$= Experimental Failure Load

$w_T$= Predicted Failure Load Using Modified Newmark's Method

$w_A$= Predicted Failure Load Using the Design Equation

Table 4.8
Modified Newmark's Method Results for 50 ft. Span Joists

| | | Test No. | Bridging Spacing (ft.) | $(kS/r)_y$ | Insulation | Exp. $w_E$ (plf) | Theoretical | | Approximate | | |
|---|---|---|---|---|---|---|---|---|---|---|---|
| | | | | | | | $w_T$ (plf) | $w_E/w_T$ | $w_A$ (plf) | $w_E/w_A$ | $w_T/w_A$ |
| Angle web | 40 psf | 50/3/40-31 | 9.90 | 100.7 | N | 264.1 | 318.3 | 0.83 | 317.7 | 0.83 | 1.00 |
| | | 50/3/40-33 | 9.90 | 101.1 | N | 367.7 | 313.0 | 1.17 | 312.4 | 1.18 | 1.00 |
| | | 50/3/40-29 | 6.30 | 62.2 | N | 422.2 | 381.5 | 1.11 | 384.0 | 1.10 | 0.99 |
| | | 50/3/40-30 | 6.30 | | | 347.6* | | | | | |
| | | 50/3/40-32 | 6.30 | 64.3 | N | 349.3 | 369.4 | 0.95 | 372.0 | 0.94 | 0.99 |
| | | 50/3/40-28 | 5.20 | | | 334.8* | | | | | |
| | | 50/3/40-27 | 4.60 | | | 334.2* | | | | | |

* Not conducted to failure

$w_E$= Experimental Failure Load

$w_T$= Predicted Failure Load Using Modified Newmark's Method

$w_A$= Predicted Failure Load Using the Design Equation

Table 4.9
Modified Newmark's Method Results for 60 ft. Span Joists

| | | Test No. | Bridging Spacing (ft.) | $(kS/r)_y$ | Insulation | Exp. $w_E$ (plf) | Theoretical | | Approximate | | |
|---|---|---|---|---|---|---|---|---|---|---|---|
| | | | | | | | $w_T$ (plf) | $w_E/w_T$ | $w_A$ (plf) | $w_E/w_A$ | $w_T/w_A$ |
| Angle web | 20 psf | 60/3/20-4 | 30.0 | 373.8 | N | 110.0 | 249.0 | 0.44 | 246.0 | 0.45 | 1.01 |
| | | 60/4/20-1 | 20.0 | 243.1 | I | 111.7 | 201.0 | 0.56 | 194.3 | 0.58 | 1.03 |
| | | 60/4/20-2 | 20.0 | 242.0 | I | 111.7 | 212.8 | 0.52 | 205.1 | 0.55 | 1.04 |
| | | 60/3/20-5 | 15.0 | 179.0 | N | 162.9 | 179.7 | 0.91 | 170.4 | 0.96 | 1.05 |
| | | 60/3/20-6 | 13.2 | 155.1 | N | 170.5 | 166.6 | 1.02 | 159.7 | 1.07 | 1.04 |
| | | 60/3/20-3 | 13.2 | 169.6 | N | 123.0 | 158.1 | 0.78 | 151.0 | 0.82 | 1.05 |
| | | 60/3/20-7 | 10.0 | 115.0 | N | 197.8 | 166.4 | 1.19 | 163.5 | 1.21 | 1.02 |
| | | 60/3/20-8 | 10.0 | 117.6 | N | 138.4 | 165.5 | 0.84 | 162.4 | 0.85 | 1.02 |
| | | 60/3/20-9 | 9.3 | 114.9 | N | 128.9 | 165.5 | 0.78 | 160.6 | 0.80 | 1.03 |
| | | 60/3/20-16 | 9.3 | 113.7 | N | 133.5 | 159.4 | 0.84 | 154.9 | 0.86 | 1.03 |
| | | 60/3/20-17 | 7.6 | 90.1 | N | 210.4 | 177.8 | 1.18 | 178.2 | 1.18 | 1.00 |
| | | 60/3/20-18 | 7.6 | 94.3 | N | 148.3 | 178.1 | 0.83 | 178.6 | 0.83 | 1.00 |
| | | 60/3/20-26 | 7.7 | 90.9 | N | 153.2 | 179.4 | 0.85 | 179.8 | 0.85 | 1.00 |
| | | 60/3/20-19 | 6.0 | 74.8 | N | 163.1 | 199.2 | 0.82 | 199.8 | 0.82 | 1.00 |
| | | 60/3/20-20 | 4.0 | 48.3 | N | 180.4 | 222.3 | 0.81 | 223.4 | 0.81 | 1.00 |
| | | 60/3/20-21 | 4.0 | 48.3 | N | 187.8 | 221.5 | 0.85 | 222.6 | 0.84 | 1.00 |
| | 40 psf | 60/3/40-10 | 10.4 | 102.4 | N | 316.5 | 277.0 | 1.14 | 276.3 | 1.14 | 1.00 |
| | | 60/3/40-24 | 7.7 | 75.0 | R | 306.6 | 315.2 | 0.97 | 315.8 | 0.97 | 1.00 |
| | | 60/3/40-25 | 7.7 | 74.4 | R | 309.1 | 323.0 | 0.96 | 323.6 | 0.96 | 1.00 |
| | | 60/3/40-23 | 4.0 | 39.4 | N | 399.3 | 372.8 | 1.07 | 373.4 | 1.07 | 1.00 |
| | | 60/3/40-22 | 4.0 | 39.4 | N | 411.8 | 372.8 | 1.10 | 373.4 | 1.10 | 1.00 |

$w_E$= Experimental Failure Load

$w_T$= Predicted Failure Load Using Modified Newmark's Method

$w_A$= Predicted Failure Load Using the Design Equation

slenderness ratio was 270.2.

50 ft. Span Tests. From Table 4.8, the ratio $w_E/w_T$ ranged from 0.83 to 1.17 for this series, bridging spacing was between 4.6 ft. and 9.9 ft. The corresponding top chord slenderness ratios ranged from 62.2 to 100.7.

60 ft. Span Tests. From Table 4.9, the ratio of $w_E/w_T$ ranged from 0.44 to 1.19 with bridging spacing varying between 4 ft. and 30 ft. for the nominal 20 psf tests. The corresponding top chord slenderness ratios ranged from 48.3 to 373.8. The ratio of $w_E/w_T$ ranged from 0.96 to 1.14 with bridging spacing between 4 ft. and 10.4 ft. for the nominal 40 psf tests. The corresponding top chord slenderness ratios ranged from 39.4 to 102.4.

## 4.4 Discussion

Comparisons of experimental to predicted failure loads have been made in the previous section using two different methods. The Clip-Frictional Force method was approximately 25% unconservative for 50 ft. and 60 ft. span angle web joists and $(kS/r)_y$ less than approximately 125. As $(kS/r)_y$ increases, the method becomes conservative. On the other hand, the method was conservative for all 40 ft. span angle and rod web joists. The degree of conservatism was about 20% higher for rod web than it was for angle web joists, this conservatism also increases with the top chord slenderness ratio $(kS/r)_y$.

The Modified Newmark's Iterative method was at most 22% unconservative for the nominal 20 psf 60 ft. span angle web joists for $(kS/r)_y$ less than approximately 200. As $(kS/r)_y$ increases above 200, the method be-

comes increasingly unconservative, this unconservatism is due to assuming that the lateral stiffness of the web members is equivalent to the lateral stiffness of a fixed-fixed column. The unconservatism due to this assumption is less than 20% for slenderness ratios less than approximately 200 because the web restraining strength provided to the top chord is small in comparison to the strength of the chord itself in that case. It is concluded that this assumption is acceptable for the slenderness ratio range allowed by the AISC and SJI codes[1,11] less than 200. On the other hand, the method was reasonably accurate for 40 ft. and 50 ft. span angle web joists (within about 15%), where $(kS/r)_y$ ranged from 62.2 to 119.6, and about 25% conservative for all 40 ft. span rod web joists.

By comparing the results from both methods, the Modified Newmark's method was found to be consistently closer to the experimental results than the Clip-Frictional Force method. Advantages and disadvantages of both methods are given below for comparison purposes.

Clip-Frictional Force Method. Advantages: 1) very simple, based mainly on statics 2) easy to automate 3) gives good results for top chord slenderness ratio in the range 50-125. Disadvantages: 1) neglects an important factor which is web restraining effect. It is noted here that this factor can not be taken into account with the clip forces because analysis of the web requires proportional loading whereas this is not the case for clip-frictional forces analysis; 2) it is an approximate method and does not have any theoretical basis; 3) axial load variation is neglected for reasons mentioned in (1); 4) very conservative for top chord slenderness ratios greater than approximately 125.

Modified Newmark's Iterative Method. Advantages: 1) gives good

results for top chord slenderness ratios below 200; 2) easy to automate; 3) it has theoretical basis; 4) considers two important factors that are believed to be essential to joist load carrying capacity, namely, web restraining effect and top chord axial load variation. Disadvantages: 1) unconservative for large top chord slenderness ratios due to the assumption that web members are completely fixed at top and bottom chord panel points. This causes the assumed lateral stiffness of the web members at panel points to be higher than their actual value. However, for small bridging spacing, the top and bottom chords become very stiff laterally and torsionally, and actual web stiffness at panel points becomes close to completely fixed.

## 4.5 Development of Design Methodology

Two analysis procedures have been developed to predict load carrying capacity of light trusses and open web steel joists supporting standing seam roof systems. The results from the second method, Modified Newmark's, resulted in better agreement with experimental results. Moreover, this method possesses a theoretical basis. It is desired now that this method be simplified for possible design applications. A design equation is developed based on the computer program given in Appenix C. The development of this equation is illustrated below.

The critical load determined by the Modified Newmark's method is typically given by Equation 4.1

$$P_{cr} = a\,(EI_y/S^2) + b\,(KS) \qquad (4.1)$$

where "a" is a factor determined from analysis, it depends on the top chord axial load variation and has a minimum value of $9.87 = \pi^2$ (Euler

buckling load for a pinned column with constant axial load), "b" is a factor that depends on the number of panel points between bridging lines, S = top chord bridging spacing at or closest to midspan, $I_y$ = moment of inertia of the top chord with respect to the vertical axis, and K = web stiffness at panel points in the top chord buckling direction.

Since "a" varies with axial load distribution along the top chord between bridging lines, and since axial load variation depends on span length, L, and bridging spacing, S, it is concluded that "a" is a function of L and S. In order to illustrate this relationship, the coefficient "a" was plotted against $(S/L)^2$; the result is shown in Figure 4.3a. Similarily, since "b" varies with the number of panel points along the top chord between bridging lines, and since the number of panel points between bridging lines varies with bridging spacing, S, span length, L, and panel point spacing, p, it is concluded that "b" is a function of S, L and p. In order to illustrate this relationship, "b" was plotted against $(S^2/Lxp)$; the result is shown in Figure 4.3b. Best fit linear polynomials for the curves shown in Figure 4.3 are

$$a = 17(S/L)^2 + 9.87 \qquad (4.2a)$$

$$b = 0.21(S^2/L\,p\,) + c \qquad (4.2b)$$

where c = 0.24 for rod web joists and c = 0.16 for angle web joists.

Predicted failure loads using Equations 4.1 and 4.2 are now compared to the predicted failure loads using the computer program based on the Modified Newmark's method and to the experimental failure loads. All comparisons are made without including a factor of safety. Results of these comparisons are given in Tables 4.7, 4.8 and 4.9 for 40 ft.,

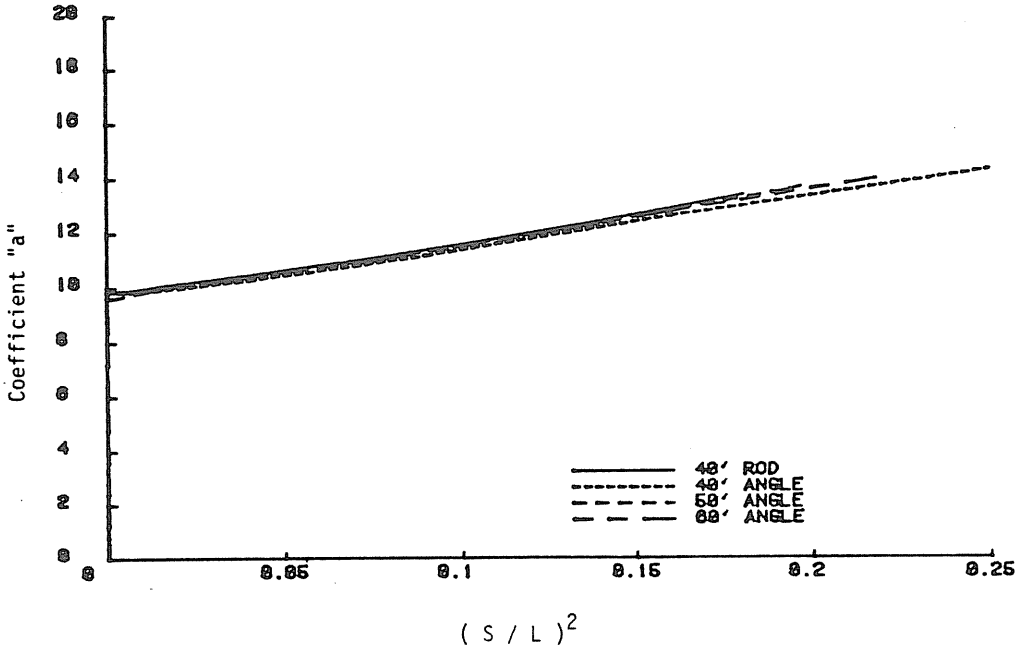


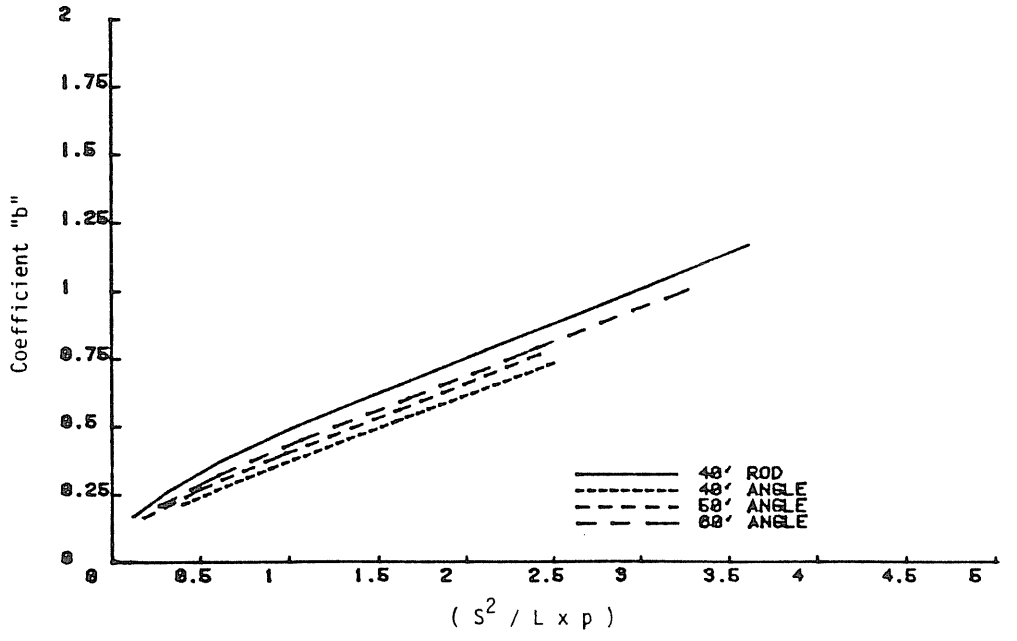


Figure 4.3 Relationship of Coeffecients "a" and "b" in Equation 4.1 to Joist Variables

50 ft. and 60 ft. span joists, respectively. In these tables, $w_T/w_A$ is the ratio of predicted failure load using the Modified Newmark's method to the predicted failure load using the design equation. An ideal case is one in which this ratio is equal to unity. A ratio greater than one indicates a conservative design equation answer and a ratio less than one indicates an unconservative answer. Also, $w_E/w_A$ is the ratio of experimental failure load to the predicted failure load using the design equation. A ratio greater than one indicates a conservative answer and a ratio less than one indicates an unconservative answer.

The ratio of $w_T/w_A$ ranged from 0.99 to 1.05 for 40 ft. span joist tests, from 0.99 to 1.00 for 50 ft. span joist tests and from 1.00 to 1.05 for 60 ft. span joist tests. This indicates an excellent agreement between the Modified Newmark's method and the design equation results. The closeness of the design equation and the Modified Newmark's answers is shown by comparing the ratios of $w_E/w_A$ and $w_E/w_T$ for 40 ft., 50 ft. and 60 ft. span joists.

From Table 4.7, the ratio $w_E/w_A$ ranged from 0.77 to 1.45 whereas $w_E/w_T$ ranged from 0.77 to 1.41 for 40 ft. span rod web joist tests. Also, the ratio $w_E/w_A$ ranged from 1.01 to 1.13 whereas $w_E/w_T$ ranged from 1.01 to 1.12 for 40 ft. span angle web joist tests. From Table 4.8, the ratio $w_E/w_A$ ranged from 0.83 to 1.18 whereas $w_E/w_T$ ranged from 0.83 to 1.17 for 50 ft. span angle web joist tests. Finally, from Table 4.9, the ratio $w_E/w_A$ ranged from 0.45 to 1.21 whereas $w_E/w_T$ ranged from 0.44 to 1.19 for 60 ft. span angle web joist tests. Thus, it is clear that equally acceptable results are obtained if the simplified design equation is used.

## 4.6 Summary

This research has studied the behavior of light trusses and open web steel joists supporting standing seam roof systems. Two methods have been developed in addition to a simplified design equation. This design equation is based on the method that was believed to be the more accurate. Predicted failure loads for open web steel joists using both methods and the design equation were compared with experimental results from tests conducted and reported by Holland and Murray at Fears Structural Engineering Laboratory at the University of Oklahoma[2]. Recommendations for the use of the proposed design procedure are given in Chapter V.

# CHAPTER V

# SUMMARY, CONCLUSIONS AND RECOMMENDATIONS

## 5.1 Summary and Conclusions

Predicted failure loads using the simplified design equation, that was developed based on the Modified Newmark's method, have been compared to experimental failure loads for various spans and for both angle and rod web joists. These predicted loads were close to the experimental loads for angle web joists for top chord slenderness ratios allowed by the different codes specifications (within 20% range). However, the predicted loads were substantially lower than the experimental loads (20% to 40%) for rod web joists. This suggests that rod web joists are stronger than angle web joists (approximately 20%).

There are two explanations to this phenomenon. First, the web in angle web joists is constructed using equal leg angles crimped at top and bottom chord panel points as is shown in Figure 1.3(a), whereas the web in rod web joists is constructed using a continuous round rod bend and welded to the top and bottom chord members as was shown in Figure 1.3(b). The continuity in rod web joists provides the top chord with stronger web stiffness at panel points. This increase in the top chord stiffness at panel points increases the top chord ultimate load carrying

capacity. The second explanation is the fact that panel point spacing is larger in angle web joists than it is in rod web joists (4 ft. in angle web, 2 ft. in rod web). A larger panel point spacing increases the difference in axial load values between any two adjacent panel points. Consequently, the stress concentration in angle web panel points is higher than it is in rod web panel points.

For both angle and rod web joists, the Modified Newmark's method becomes unconservative as top chord slenderness ratio increases above approximatily 200. The reason for this unconservatism was explained in Chapter IV, however, such large slenderness ratios are not allowed by the SJI and the AISC specifications.

The results of the design equation developed in Chapter IV based on the Modified Newmark's method did not differ by more than 5% for all tests studied from the "exact" results obtained using the computer program in Appendix C.

## 5.2 Recommendations

The Modified Newmark's results have been shown to provide good agreement with the experimental results. Moreover, the results of the design equation developed based on this method were almost identical to the "exact" method results. Therefore, it is concluded that the design equation developed in Chapter IV can be used in place of the Modified Newmark's method. The results of this design equation can be expected to be good for angle web joists and about 20 to 30% conservative for rod web joists.

Finally, in order to strengthen angle web joists, it is suggested

that a 5 to 8 in. round rod be welded to the top chord angles at panel points. This round rod will provide the continuity that was lacked in angle web joists, see Figure 5.1.

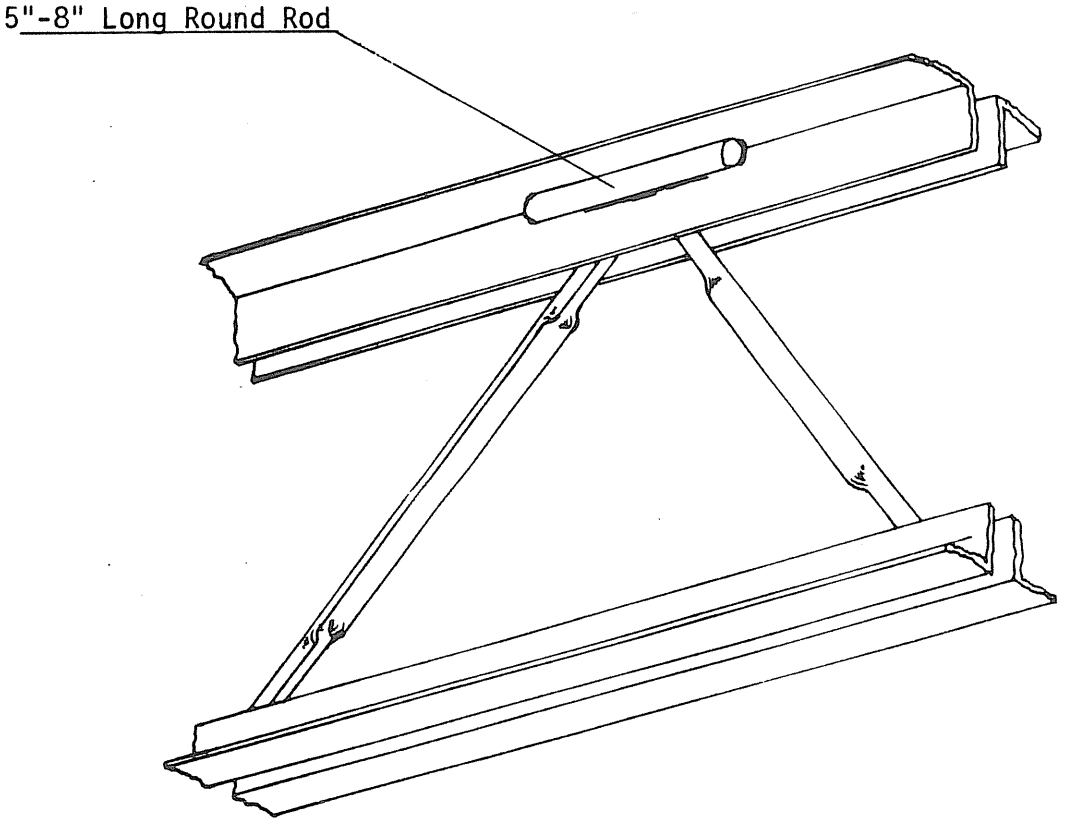


Figure 5.1 Angle Web Joist Reinforcement at Top Chord Panel Point

## REFERENCES


1. Steel Joists and Joist Girders: VULCRAFT Division of NUCOR Corporation, 1979.

2. Holland, Mark V. and Murray, Thomas M., "Behavior of Steel Joists Supporting Standing Seam Roof Systems", Final Report submitted to VULCRAFT Division of NUCOR Corporation, Fears Structural Engineering Laboratory, The University of Oklahoma, Report No. FSEL/VULCRAFT 83-01, October 1983, 67 pages.

3. Specification for the design, Fabrication and Erection of Strucutral Steel for Buildings. American Institute of Steel Construction, 1978.

4. Cold-Formed Steel Design Manual. American Iron and Steel Institute, 1980.

5. Lenzen, K. H. "Pilot Study-The Applicability of the AISC Formula to the Top Chords of Steel Joists", Studies in Engineering Mechanics, University of Kansas, Report No. 19, November 1965.

6. Hribar, J. A., "Investigation of the Elastic Lateral Stability of Open Web Steel Joists and the Spacing of Rows of Bridging", Final Report, Revised Edition, Carnegie Institute of Technology, June 1966.

7. Steel Joist Institute Technical Digest. "Spacing of Bridging for Open Web Steel Joists", No. 2, September 1970.

8. Salmon, C. G. and Johnson, J. E., Steel Structures Design and Behavior. New York: Harper and Row 1980.

9. Godden, W. G., Numerical Analysis of Beam and Column Structures. Englewood Cliffs, New Jersey: Prentice Hall, 1965.

10. Newmark, N. M., "Numerical Procedure for Computing Deflections and Buckling Loads", ASCE Journal, vol. 108, Paper No. 2202, 1943, pp. 1161-1234

# APPENDIX A

## MODIFIED NEWMARK'S METHOD EXAMPLE CALCULATIONS

The configuration of Test 40/3/20-14W of Reference 2 is used to demonstrate the required calculations, using Modified Newmark's Iterative procedure method. The required data is as follows:

Material Data: E=29,000 ksi, Fy=57.9 ksi

Joist Data: $I_x$=118.05 $in.^4$, d=18.9 in.

Top Chord Data: $I_y$=0.551 $in.^4$, A=0.68 $in.^2$

Bridging Data: S=10 ft.

Web Data: 9/16 in. $\phi$, $L_w$=23.32 in., $I_w$=0.00491, K=0.2695

From the bridging spacing, the top chord and the top chord loading is as given below:

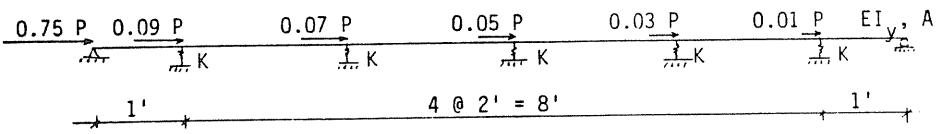


1) Axial Force Analysis:

The analysis is initiated by assuming a sinusoidal buckled shape (with amplitude e), the chord is divided into 10 segments as shown below:

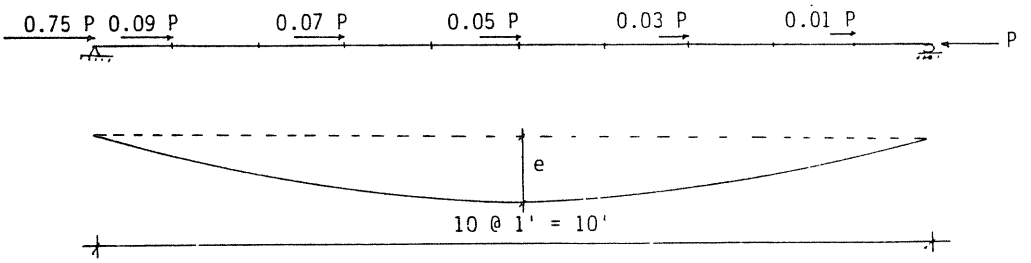


First Cycle

| | | | | | | | | | | | | |
|---|---|---|---|---|---|---|---|---|---|---|---|---|
| $y_a$ | 0 | 0.31 | 0.59 | 0.81 | 0.95 | 1.00 | 0.95 | 0.81 | 0.59 | 0.31 | 0 | e |
| M | 0 | 0.21 | 0.44 | 0.60 | 0.71 | 0.75 | 0.68 | 0.53 | 0.30 | 0.0 | 0 | eP |
| y" | 0 | 0.21 | 0.44 | 0.60 | 0.71 | 0.75 | 0.68 | 0.53 | 0.30 | 0.0 | 0 | $eP/EI_y$ |
| Y" | 0 | 2.54 | 5.21 | 7.15 | 8.45 | 8.89 | 8.08 | 6.28 | 3.53 | 0.30 | 0 | $ePh/12EI_y$ |
| y' | 25.22 | 22.68 | 17.47 | 10.32 | 1.87 | -7.02 | -15.1 | -21.38 | -24.91 | -25.2 | | $ePh^2/12EI_y$ |

| | | | | | | | | | | | | |
|---|---|---|---|---|---|---|---|---|---|---|---|---|
| $y_c$ | 0 | 25.22 | 47.9 | 65.37 | 75.69 | 77.56 | 70.54 | 55.44 | 34.06 | 9.15 | -15.7 | $ePh^2/12EI_y$ |
| correction | 0 | 1.57 | 3.14 | 4.71 | 6.28 | 7.85 | 9.42 | 10.99 | 12.56 | 14.13 | 15.7 | |
| $y_c$ | 0 | 26.79 | 51.04 | 70.08 | 81.97 | 85.41 | 79.96 | 66.43 | 46.62 | 23.28 | 0 | $ePh^2/12EI_y$ |
| Normalized $y_c$ | 0 | 0.31 | 0.60 | 0.82 | 0.96 | 1.0 | 0.94 | 0.78 | 0.55 | 0.27 | 0 | |

Second Cycle

| | | | | | | | | | | | | |
|---|---|---|---|---|---|---|---|---|---|---|---|---|
| $y_a$ | 0 | 0.31 | 0.60 | 0.82 | 0.96 | 1.0 | 0.94 | 0.78 | 0.55 | 0.27 | 0 | e |
| M | 0 | 0.25 | 0.51 | 0.71 | 0.85 | 0.91 | 0.87 | 0.72 | 0.52 | 0.25 | 0 | eP |
| y" | 0 | 0.25 | 0.51 | 0.71 | 0.85 | 0.91 | 0.87 | 0.72 | 0.52 | 0.25 | 0 | $eP/EI_y$ |
| Y" | 0 | 3.01 | 6.06 | 8.46 | 10.12 | 10.82 | 10.33 | 8.59 | 6.17 | 3.02 | 0 | $ePh/12EI_y$ |
| y' | 33.29 | 30.28 | 24.22 | 15.76 | 5.64 | -5.18 | -15.51 | -24.1 | -30.27 | -33.29 | | $ePh^2/12EI_y$ |
| $y_c$ | 0 | 33.29 | 63.57 | 87.79 | 103.6 | 109.2 | 104.0 | 88.50 | 64.4 | 34.13 | 0.84 | $ePh^2/12EI_y$ |
| correction | 0 | -0.08 | -0.17 | -0.25 | -0.34 | -.42 | -0.50 | -0.59 | -0.67 | -0.76 | -0.84 | |
| $y_c$ | 0 | 33.21 | 63.4 | 87.54 | 103.2 | 108.8 | 103.5 | 87.9 | 63.73 | 33.37 | 0 | $ePh^2/12EI_y$ |
| Normalized $y_c$ | 0 | 0.31 | 0.58 | 0.81 | 0.95 | 1.00 | 0.95 | 0.81 | 0.59 | 0.31 | 0 | |

Third Cycle

| | | | | | | | | | | | | |
|---|---|---|---|---|---|---|---|---|---|---|---|---|
| $y_a$ | 0 | 0.31 | 0.58 | 0.81 | 0.95 | 1.00 | 0.95 | 0.81 | 0.59 | 0.31 | 0 | e |
| M | 0 | 0.25 | 0.49 | 0.70 | 0.84 | 0.91 | 0.88 | 0.75 | 0.56 | 0.29 | 0 | eP |
| y" | 0 | 0.25 | 0.49 | 0.70 | 0.84 | 0.91 | 0.88 | 0.75 | 0.56 | 0.29 | 0 | $eP/EI_y$ |
| Y" | 0 | 2.99 | 5.85 | 8.33 | 10.01 | 10.82 | 10.46 | 8.94 | 6.64 | 3.46 | 0 | $ePh/12EI_y$ |
| y' | 33.75 | 30.76 | 24.91 | 16.58 | 6.57 | -4.25 | -14.71 | -23.65 | -30.29 | -33.75 | | $ePh^2/12EI_y$ |
| $y_c$ | 0 | 33.75 | 64.51 | 89.42 | 106.0 | 112.6 | 108.3 | 93.61 | 69.96 | 39.67 | 5.92 | $ePh^2/12EI_y$ |
| correction | 0 | -0.59 | -1.18 | -1.78 | -2.37 | -2.96 | -3.55 | -4.14 | -4.74 | -5.33 | -5.92 | |
| $y_c$ | 0 | 33.16 | 63.33 | 87.64 | 103.63 | 109.6 | 104.77 | 89.47 | 65.22 | 34.34 | 0 | $ePh^2/12EI_y$ |
| Normalized $y_c$ | 0 | 0.30 | 0.58 | 0.80 | 0.95 | 1.00 | 0.96 | 0.82 | 0.60 | 0.31 | 0 | |

This level of accuracy is acceptable. Therefore, the calculations are stopped

2) Spring Force Analysis:

The second part of the problem is the web effect, simulated by a series of springs acting on the top chord as shown below:

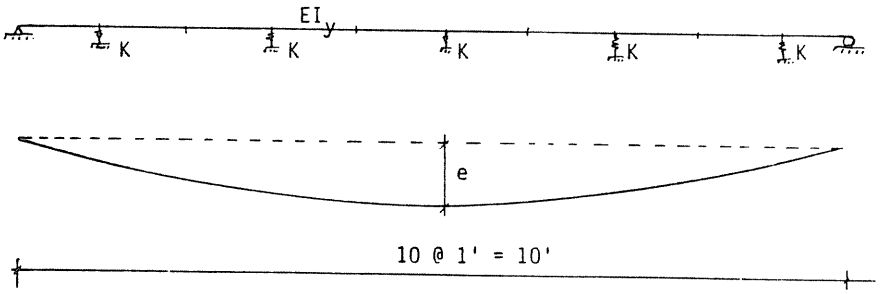


First Cycle

| | | | | | | | | | | | | |
|---|---|---|---|---|---|---|---|---|---|---|---|---|
| $y_a$ | 0 | 0.31 | 0.59 | 0.81 | 0.95 | 1.00 | 0.95 | 0.81 | 0.59 | 0.31 | 0 | e |
| M | 0 | -1.62 | -2.93 | -4.24 | -4.74 | -5.24 | -4.74 | -4.24 | -2.93 | -1.62 | 0 | eKh |
| y" | 0 | -1.62 | -2.93 | -4.24 | -4.74 | -5.24 | -4.74 | -4.24 | -2.93 | -1.62 | 0 | $eKh/EI_y$ |
| Y" | 0 | -9.41 | -17.58 | -24.63 | -28.44 | -30.44 | -28.44 | -24.63 | -17.58 | -9.41 | 0 | $eKh^2/6EI_y$ |
| y' | -95.28 | -85.87 | -68.29 | -43.66 | -15.22 | 15.22 | 43.66 | 68.29 | 85.87 | 95.28 | | $eKh^3/6EI_y$ |
| $y_c$ | 0 | -95.28 | -181.2 | -249.4 | -293.1 | -308.3 | -293.1 | -249.4 | -181.2 | -95.28 | 0 | $eKh^3/6EI_y$ |
| Normalized $y_c$ | 0 | -0.31 | -0.59 | -0.81 | -0.95 | -1.00 | -0.95 | -0.81 | -0.59 | -0.31 | 0 | |

This level of accuracy is acceptable, therefore, the calculation is stopped. The buckling load can now be determined using the results from the third cycle, results from the axial force analysis, and the results of the frist cycle of the spring force analysis. Equating the assumed deflection at midspan to the summation of the calculated deflections at midspan for the axial and spring forces gives:

$$1.0\ e = 109.6\ ePh^2/12EI_y - 308.3\ eKh^3/6EI_y$$

but since the column is divided into 10 regions, h=S/10, thus,

$$P_E = 10.95\ EI_y/S^2 + 0.56\ KS$$

where $P_E$= elastic buckling load, S = bridging spacing, K = web lateral stiffness at panel point. Substituting numerical values for E, $I_y$, S and K into $P_E$ equation results in

$$P_E = 30.26 \text{ kips}$$

This load is compared with the proportaional limit load where the latter is defined in Equation 3.21, $P_p$=0.5x0.68x57.9=19.69 kips. Since $P_E$ is greater than $P_p$ then Equation 3.20b applies:

$$P_{cr} = (57.9 \times 0.68) - (57.9 \times 0.68)^2/4 \times 30.26 = 26.57 \text{ kips}$$

Finally, the equivalent uniform load applied on the joist is calculated using Equation 3.8 which gives,

$$w = 8 \times 26.57 \times 18.9/(10 \times 12)^2 = 0.0174 \text{ k/ft} = 209.2 \text{ lb/ft}$$

Note that this result differs slightly from the result reported in Table 4.7; this is due to the fact that the East side joist in Test 14 had a lower predicted failure load than the West side joist.

# APPENDIX B

## CLIP-FRICTIONAL FORCE METHOD COMPUTER PROGRAM

```
      CHARACTER*15 NAME
      REAL KLRY,PP,PT
      INTEGER TYPE
      DO 1001 KKK=1,92
      READ(5,15)TYPE,NAME
15    FORMAT(I1,A15)
      IF(TYPE.EQ.1)THEN
      READ*,SPAN,SPACE,X,Y,D,A,FY,Q,ACTUAL
      ELSE
      READ*,SPAN,SPACE,X,Y,YY,D,A,FY,Q,ACTUAL
      END IF
* CALCULATE THE NUMBER OF CLIPS BETWEEN BRIDGING LINES:
      NCLIP=(SPACE/24.)-1
      KLRY=SPACE/(SQRT(Y/A))
      AXIAL=ACTUAL*(SPAN**2)/(D*8*12)
      VALUE=NCLIP/2.0
      NNN=VALUE
      VALUE1=VALUE-NNN
      SUM1=0.0
      SUM2=0.0
* CALCULATE THE ELASTIC BUCKLING LOAD:
      IF(VALUE1.NE.0.0)GO TO 400
      DO 30 I=1,NNN
      SUM1=SUM1+12+24*(I-1)
30    CONTINUE
      DO 90 I=1,NNN
      SUM2=SUM2+2*SIN((SPACE/2-(12+24*(I-1)))*3.14159/SPACE)
90    CONTINUE
      BB=2*(SPACE**3)*SUM2/((3.14159**4)*29000000*Y)
      GO TO 11
400   DO 50 I=1,NNN
      SUM1=SUM1+24*I
50    CONTINUE
      DO 100 I=1,NNN
      SUM2=SUM2+2*SIN((SPACE/2-(24*(I-1)))*3.14159/SPACE)
100   CONTINUE
      SUM2=SUM2+1
      BB=2*(SPACE**3)*SUM2/((3.14159**4)*29000000*Y)
* INCORPORATE THE INELASTIC BUCKLING EFFECT:
11    PP=(SUM1-NCLIP*SPACE/4)/BB
      PT=((9.87*29000000*Y)/(SPACE**2))-PP
      PE=FY*.5*A
      IF(PT.GT.PE)THEN
      PT=PE*2-(((PE*2)**2)/(4*PT))
      ELSE
      PT=PT
      END IF
      UNI=12*PT*8*D/(SPAN**2)
      IF(TYPE.EQ.1)THEN
      WRITE(6,60)NAME
60    FORMAT(7X,"   TEST : ",A11,20X,"ROD")
      PRINT*,"-------------------------------------------------------------------"
      PRINT*,"    KL/R        IY       THEOR.      EXP.       AXIAL        IY/IEFF"
      PRINT*,"              (IN.4)     W(PLF)     W(PLF)     (KIP)"
      PRINT*,"-------------------------------------------------------------------"
      PRINT*," "
      WRITE(6,70)KLRY,Y,UNI,ACTUAL,AXIAL/1000,ACTUAL/UNI
70    FORMAT(3X,F5.1,5X,F5.3,5X,F5.1,6X,F5.1,5X,F6.3,8X,F4.2)
      PRINT*," "
      PRINT*,"-------------------------------------------------------------------"
      WRITE(6,2001)SPACE/12.
2001  FORMAT("  BRIDGING SPACING = ",F4.1,/////)
      ELSE
      WRITE(6,80)NAME
80    FORMAT(7X,"   TEST : ",A11,23X,"ANGLE")
      PRINT*,"-------------------------------------------------------------------"
      PRINT*,"    KLRY        IY       THEOR.      EXP        AXIAL        IY/IEFF"
      PRINT*,"              (IN.4)     W(PLF)     W(PLF)     (KIP)"
      PRINT*,"-------------------------------------------------------------------"
      PRINT*," "
      WRITE(6,101)KLRY,Y,UNI,ACTUAL,AXIAL/1000,ACTUAL/UNI
101   FORMAT(3X,F6.1,5X,F5.3,5X,F5.1,6X,F5.1,5X,F6.3,8X,F4.2)
      PRINT*," "
      PRINT*,"-------------------------------------------------------------------"
      WRITE(6,3001)SPACE/12
3001  FORMAT("  BRIDGING SPACING = ",F4.1,/////)
      END IF
1001  CONTINUE
      STOP
      END
```

# APPENDIX C

# MODIFIED NEWMARK'S METHOD COMPUTER PROGRAM

```
* THIS PROGRAM CALCULATES THE CRITICAL BUCKLING LOAD OF A TOP CHORD
* IN A STEEL JOIST, TAKING INTO ACCOUNT THE AXIAL LOAD VARIATION ALONG
* THE TOP CHORD AND THE WEB EFFECT BY ASSUMING THAT THE WEB MEMBERS
* COULD BE REPRESENTED BY A SERIES OF SPRINGS AT THE PANEL POINTS.
      DIMENSION YYY(50),P(50),NODE(50),Y(50),W1(50),YY1(50),YYY1(50)
      DIMENSION YY2(50)
      REAL MOM1(50)
      CHARACTER*15 NAME
* READ THE TEST NAME :
      READ(5,11)NAME
11    FORMAT(A15)
* READ THE FOLLOWING: - NLOAD = NUMBER OF LOADS
*                     - NNODE = NUMBER OF NODES
*                     - STIFF = 1 IF THE EFFECT OF WEB IS CONSIDERED
*                             = 0 IF THE WEB EFFECT IS NEGLECTED
*                     - XX    = MOMENT OF INERTIA OF JOIST ABOUT STRONG AXIS IN
*                     - YY    = LATERAL MOMENT OF INERTIA OF TOP CHORD IN (IN 4)
*                     - D     = EFFECTIVE DEPTH OF JOIST IN ( IN )
*                     - A     = AREA OF TOP CHORD IN ( IN )
*                     - FY    = YIELD STRENGTH OF STEEL USED IN ( KSI )
*                     - WEB   = LATERAL STIFFNESS OF A PANEL POINT IN ( K/IN )
*                     - S     = BRIDGING SPACING IN ( FT )
*                     - SPAN  = TOTAL LENGTH OF JOIST IN ( FT )
*                     - EXP   = EXPERIMENTAL RESULT IN ( PLF )
      READ*,NLOAD,NNODE,STIFF,XX,YY,D,A,FY,WEB,S,SPAN,EXP
      DO 15 I=1,NNODE+1
      P(I)=0.0
      MOM1(I)=0.0
      Y(I)=0.0
      NODE(I)=0.0
      W1(I)=0.0
      YY1(I)=0.0
      YYY1(I)=0.0
      YYY(I)=0.0
15    CONTINUE
      NUMBER=1
      NUMB=1
* READ VALUES OF LOADS AND THEIR LOCATIONS; VALUE OF EACH LOAD
* IS ENTERED AS "A" WHERE "A" IS EQUAL TO THE RATIO OF THE ENTERED LOAD
* OVER THE SUMMATION OF ALL APPLIED LOADS; THE COORDINATE OF
* EACH LOAD IS ENTERED AS THE NODAL POINT NUMBER WHERE THE LOAD
* IS APPLIED :
      READ*,(P(I),I=1,NLOAD)
      READ*,(NODE(I),I=1,NLOAD)
* ENTER THE NODAL POINT NUMBER THAT YOU WANT TO CHECK THE
* DEFLECTIONS AGAINST AND THE VALUE OF EPSILON ( FOR ACCURACY )
* REQUIRED :
      READ*,N,EPSIL
* CALCULATE THE VALUES OF INITIAL DEFLECTION AT EACH NODAL POINT
* NOTE THAT THE VALUES OF THESE INITIAL DEFLECTIONS REPRESENT
* ONLY THE RELATIVE DISPLACEMENT OF THESE POINTS AND NOT THE
* ACTUAL DEFLECTIONS AT THE COLUMN. THEREFORE, THESE NUMBERS
* ARE DIMENSIONLESS . THE ASSUMED DEFLECTION MODE IS A SINE CURVE :
      DO 10 I=1,NNODE+1
      Y(I)=SIN(3.14159*(I-1)/NNODE)
10    CONTINUE
* NORMALIZE THE ASSUMED DEFLECTIONS USING THE POINT N AS A PIVOT
* POINT :
      AAA=Y(N)
      DO 370 I=1,NNODE+1
      YY2(I)=Y(I)/AAA
      Y(I)=Y(I)/AAA
370   CONTINUE
      PRINT*,"THE ASSUMED BUCKLING MODE WAS :"
      DO 180 I=1,NNODE+1
      WRITE(6,190)I,Y(I)
190   FORMAT("       Y (",I2,") = ",F7.4)
180   CONTINUE
      GO TO 20
* REPLACE VALUES OF NODAL DISPLACEMENTS BY THE NEW VALUES
* DERIVED , AND DO THE NEXT ITERATION:
25    NUMBER=NUMBER+1
      DO 35 I=1,NNODE+1
      Y(I)=YYY(I)
35    CONTINUE
*
* 1- CALCULATE THE BUCKLING MODE DUE TO THE AXIAL FORCE :
*
* CALCULATE THE MOMENTS DUE TO AXIAL FORCES
20    DO 40 I=1,NNODE+1
      MOM1(I)=0.0
      DO 50 J=1,NLOAD
      IF(NODE(J).GE.I)GO TO 50
      IF (I.EQ.1)THEN
      MOM1(I)=0.0
      ELSE
      NN=NODE(J)
      MOM1(I)=MOM1(I)+(Y(I)-Y(NN))*P(J)
      END IF
50    CONTINUE
40    CONTINUE
* CALCULATE SHEAR FORCES AT THE SUPPORTS
      SHEAR1=0.0
      DO 60 I=1,NLOAD
      NN=NODE(I)
      SHEAR1=SHEAR1+P(I)*Y(NN)
60    CONTINUE
      SHEAR1=SHEAR1/NNODE
* ADD MOMENTS DUE TO SHEAR TO ALL NODAL POINTS:
      DO 70 I=1,NNODE+1
      MOM1(I)=MOM1(I)+SHEAR1*(I-1)
70    CONTINUE
* CALCULATE NODAL CONCENTRATION OF Y" USING EQUAL PARABOLIC FORMULA
* FOR THE MOMENTS RESULTING FROM AXIAL FORCES
      DO 80 I=1,NNODE+1
      W1(I)=MOM1(I-1)+10.*MOM1(I)+MOM1(I+1)
80    CONTINUE
```

```
      W1(1)=0.0
      W1(NNODE+1)=0.0
      SUM1=0.0
      DO 85 I=1,NNODE+1
      SUM1=SUM1+W1(I)
85    CONTINUE
C CALCULATE VALUE OF Y0; AND DEFLECTION INCREMENTS :
      AA1=SUM1/2.0
      DO 90 I=1,NNODE
      YY1(I)=(AA1-W1(I))
      AA1=YY1(I)
90    CONTINUE
C CALCULATE DERIVED DEFLECTIONS :
      AA1=0.0
      YYY1(1)=0.0
      DO 100 I=2,NNODE+1
      YYY1(I)=AA1+YY1(I-1)
      AA1=YYY1(I)
100   CONTINUE
C ADD CORRECTIONS TO DERIVED DEFLECTIONS :
      AA1=YYY1(NNODE+1)
      DO 110 I=1,NNODE+1
      FACT1=AA1*(I-1)/NNODE
      YYY1(I)=YYY1(I)-FACT1
110   CONTINUE
C NORMALIZE THE DERIVED DEFLECTION BY USING DEFLECTION AT POINT N
C AS A PIVOT POINT
      CCC=YYY1(N)
      DO 115 I=1,NNODE+1
      YYY(I)=YYY1(I)/CCC
115   CONTINUE
C CHECK IF THE ALLOWABLE ACCURACY HAS BEEN REACHED :
      DO 150 I=1,NNODE+1
      CONST=ABS(YYY(I)-Y(I))
      IF(CONST.GT.EPSIL)GO TO 25
150   CONTINUE
      PRINT*,"THE CALCULATED BUCKLING MODE IS :"
      DO 160 I=1,NNODE+1
      WRITE(6,170)I,YYY(I)
170   FORMAT("      Y (",I2,") = ",F7.4)
160   CONTINUE
C
C 2- CALCULATE THE BUCKLING MODE DUE TO THE ELASTIC SPRINGS(WEB EFFECT)
C
C USE THE SAME INITIAL BUCKLING MODE THAT WAS USED IN AXIAL LOAD ANALYSIS :
      DO 220 I=1,NNODE+1
      Y(I)=YY2(I)
220   CONTINUE
      GO TO 350
C REPLACE VALUES OF NODAL DISPLACEMENT BY THE NEW VALUES DERIVED,
C AND DO THE NEXT ITERATION :
340   NUMB=NUMB+1
      DO 360 I=1,NNODE+1
      Y(I)=YYY(I)
360   CONTINUE
C CALCULATE THE MOMENTS DUE TO SPRING FORCES:
350   DO 230 I=1,NNODE+1
      MOM1(I)=0.0
      DO 240 J=1,NLOAD
      IF (NODE(J).GE.I) GO TO 240
      IF (I.EQ.1) THEN
      MOM1(I)=0.0
      ELSE
      NN=NODE(J)
      MOM1(I)=MOM1(I)-Y(NN)*(I-NN)
      END IF
240   CONTINUE
230   CONTINUE
C CALCULATE SHEAR FORCES AT THE SUPPORTS
      SHEAR2=0.0
      DO 250 I=1,NLOAD
      NN=NODE(I)
      SHEAR2=SHEAR2+Y(NN)*(NNODE+1-NN)
250   CONTINUE
      SHEAR2=SHEAR2/NNODE
C ADD MOMENTS DUE TO SHEAR TO ALL NODAL POINTS
      DO 260 I=1,NNODE+1
      MOM1(I)=MOM1(I)+SHEAR2*(I-1)
260   CONTINUE
C CALCULATE NODAL CONCENTRATION OF Y" USING UNEQUAL TRAPAZOIDAL
C FORMULA FOR THE MOMENTS RESULTING FROM THE WEB FORCES :
      DO 270 I=1,NNODE+1
      W1(I)=MOM1(I-1)+4.*MOM1(I)+MOM1(I+1)
270   CONTINUE
      W1(1)=0.0
      W1(NNODE+1)=0.0
      SUM2=0.0
      DO 280 I=1,NNODE+1
      SUM2=SUM2+W1(I)
280   CONTINUE
C CALCULATE VALUE OF Y0; AND DEFLECTION INCREMENTS :
      AA2=SUM2/2.0
      DO 290 I=1,NNODE
      YY1(I)=(AA2-W1(I))
      AA2=YY1(I)
290   CONTINUE
C CALCULATE DERIVED DEFLECTION :
      AA2=0.0
      YYY1(1)=0.0
      DO 300 I=2,NNODE+1
      YYY1(I)=AA2+YY1(I-1)
      AA2=YYY1(I)
300   CONTINUE
C ADD CORRECTIONS TO DERIVED DEFLECTIONS :
      AA2=YYY1(NNODE+1)
      DO 310 I=1,NNODE+1
      FACT2=AA2*(I-1)/NNODE
```

```
      YYY1(I)=YYY1(I)-FACT2
310   CONTINUE
* NORMALIZE THE DERIVED DEFLECTIONS BY USING DEFLECTION AT POINT N
* AS A PIVOT POINT :
      DDD=YYY1(N)
      DO 320 I=1,NNODE+1
      YYY(I)=YYY1(I)/DDD
320   CONTINUE
* CHECK IF THE ALLOWABLE ACCURACY HAS BEEN REACHED :
      DO 330 I=1,NNODE+1
      CONST=ABS(YYY(I)-Y(I))
      IF(CONST.GT.EPSIL) GO TO 340
330   CONTINUE
      WRITE(6,175)NAME
175   FORMAT("TEST : ",A15)
      VALUE1=(12.*(NNODE**2))/CCC
      IF(STIFF.EQ.0.0)THEN
      PRINT*,"THE WEB STIFFNESS IS NEGLECTED"
      VALUE2=0.0
      ELSE
      PRINT*,"THE WEB STIFFNESS IS CONSIDERED"
      VALUE2=(2.*DDD)/(NNODE*CCC)
      END IF
* INCORPORATE THE INELASTIC BUCKLING USING THE CRC FORMULA:
      VAL1=(VALUE1*29000.*YY)/((S*12)**2)
      VAL2=VALUE2*WEB*S*12
      CRITIC=VAL1*VAL2
      ELASTC=FY*A*.5
      IF(CRITIC.GT.ELASTC) THEN
      EULER=(FY*A)-(((FY*A)**2)/(CRITIC*4))
      ELSE
      EULER=CRITIC
      END IF
      W=W*EULER*D*12000/((SPAN*12)**2)
      RATIO=EXP/W
      PRINT*,"-------------------------------------------------------------
      PRINT*,"  EI/L**2       KL       P CR        W        EXP       EXP/THEO
      PRINT*,"                          (KIP)     (PLF)    (PLF)
      PRINT*,"-------------------------------------------------------------
      WRITE(6,210)VALUE1,VALUE2,EULER,W,EXP,RATIO,NUMBER
210   FORMAT(4X,F6.3,4X,F6.3,3X,F6.2,3X,F5.1,3X,F5.1,6X,F5.2,9X,I3)
      PRINT*,"-------------------------------------------------------------
      STOP
      END
```